Cu(I) and Ag(I) complexes with a new type of rigid tri-dentate N,P,P-ligand showing highly efficient TADF and remarkable OLED performance

Journal:	*Chemistry of Materials*
Manuscript ID	Draft
Manuscript Type:	Article
Date Submitted by the Author:	n/a
Complete List of Authors:	Klein, Marius; Philipps-Universitat Marburg, Chemistry Department Rau, Nicholas; Philipps-Universitat Marburg Wende, Mirco; Philipps-Universitat Marburg Sundermeyer, Jörg; Philipps-Universitat Marburg, Chemistry Department Cheng, Gang; The University of Hong Kong, Chemistry Che, Chi-Ming; University of Hong Kong, Chemistry Schinabeck, Alexander; Universitat Regensburg Yersin, Hartmut; Universitat Regensburg, Institut für Physikalische Chemie

Cu(I) and Ag(I) complexes with a new type of rigid tri-dentate N,P,P-ligand showing highly efficient TADF and remarkable OLED performance

Marius Klein[a], Nicholas Rau[a], Mirco Wende[a], Jörg Sundermeyer*[a], Gang Cheng* [b,c], Chi-Ming Che*[b,c], Alexander Schinabeck[d], Hartmut Yersin*[d]

[a] Fachbereich Chemie und Wissenschaftliches Zentrum für Materialwissenschaften, Philipps-Universität Marburg, Hans-Meerwein-Straße 4, 35043 Marburg, Germany

[b] State Key Laboratory of Synthetic Chemistry, HKU-CAS Joint Laboratory on New Materials, Department of Chemistry, The University of Hong Kong, Pokfulam Road, Hong Kong SAR, China

[c] HKU Shenzhen Institute of Research and Innovation, Shenzhen 518053, China

[d] Institute for Physical Chemistry, University of Regensburg, 93040 Regensburg, Germany

ORCID

Marius Klein: 0000-0001-9738-2567

Jörg Sundermeyer: 0000-0001-8244-8201

Chi-Ming Che: 0000-0002-2554-7219

Gang Cheng: 0000-0001-8081-8205

Alexander Schinabeck: 0000-0003-1039-7673

Hartmut Yersin: 0000-0003-3216-1370

E-Mail addresses of the corresponding authors:

Jörg Sundermeyer: jsu@staff.uni-marburg.de

Gang Cheng: ggcheng@hku.hk

Chi-Ming Che: cmche@hku.hk

Hartmut Yersin: hartmut.yersin@ur.de

TOC

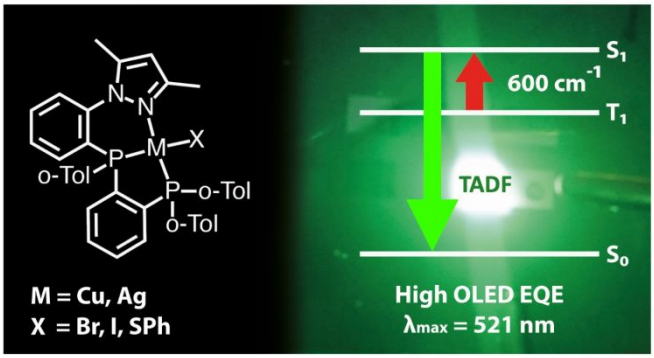

TOC text

Neutral blue to yellow brightly luminescent copper and silver complexes with a new rigid tri-dentate N,P,P ligand (dmpzpp) were prepared and their crystal structures, TD-DFT electronic structures, as well as their phosphorescence and thermally activated delayed fluorescence (TADF) properties studied in detail between $1.7 \leq T \leq 300$ K, giving $\Delta E(S_1\text{-}T_1)$, $k(S_1\text{-}S_0)$, τ(phos), k^{nr}(phos), τ(TADF), k^{nr}(TADF), ΔE(ZFS), and triplet substate decay times. Sublimable Cu(dmpzpp)I was applied for OLED fabrication affording EQE of 16.4%.

Abstract

Neutral Cu(I) and Ag(I) complexes with a new rigid tri-dentate N,P,P ligand (dmpzpp, 3,5-dimethyl-1-(2-((2-(di-*o*-tolyl)phosphanyl)(*o*-tolyl)-phosphanyl)phenyl)-1*H*-pyrazole), giving Cu(dmpzpp)Cl **6**, Cu(dmpzpp)Br **7**, Cu(dmpzpp)I **8**, Cu(dmpzpp)SPh **9**, and Ag(dmpzpp)I **10** with SPh = thiophenolato, were prepared and their crystal structures, TD-DFT electronic structures, and phosphorescence as well as thermally activated delayed fluorescence (TADF) properties studied in detail. The photo-luminescence quantum yields Φ_{PL} lie between 70 and 90% with emission colors from blue to yellow. **9** with very bulky ligands showing Φ_{PL} = 90% was used for detailed emission studies from T = 1.7 to 300 K. Up to T ≈ 70 K, **9** shows

only long-lived phosphorescence with a radiative decay time of T_1 of τ^r(phos) = 1 ms due to weak spin-orbit coupling. Accordingly, the zero-field splittings of T_1 in three substates is < 1cm^{-1} (0.1 meV) with individual decay times of 2400, 2250, and 292 µs. Presumably, the phosphorescence is essentially induced by spin-vibronic mechanisms. Up to T = 300 K, the radiative decay time decreases by more than two orders of magnitude to τ^r(TADF) = 5.6 µs due to the TADF effect. This short decay time is determined by the small gap of $\Delta E(S_1\text{-}T_1)$ = 600 cm^{-1} (74 meV) and the fast radiative $S_1 \rightarrow S_0$ rate of $1.1 \cdot 10^7$ s^{-1} (91 ns). For fabrication of an OLED device, we applied sublimable **8** using a co-host device structure and a concentration of **8** of 2 wt% resulting in a green-emitting OLED showing CIE coordinates of (0.33; 0.52), high external quantum efficiency of up to EQE = 16.4%, and high luminance of almost 10000 cd m^{-2}. Strategies for designing compounds giving higher EQE are presented.

Introduction

Fundamental research of organo-transition metal compounds was strongly stimulated by their potential or meanwhile already realized commercial application as emitters in organic light emitting diodes (OLEDs). As a consequence, extensive material research was triggered and important new compounds and exciton harvesting mechanisms were developed. Hence, a large number of materials was characterized photophysically as well as with respect to their OLED use.[1-16] For an efficient OLED device, it is essential that 100% of the singlet (25%) and triplet (75%) excitons[5,9,17,18] formed in the emission layer are harvested and converted into light. This is only successful with adequately designed emitter compounds. The original OLED concept[19] that, based on "normal" fluorescent molecules, only exploits the singlet excitons. However, different exciton harvesting mechanisms have been developed meanwhile that improve the OLED efficiency dramatically: (i) By applying Ir(III) or Pt(II) complexes, for example, showing relatively fast and efficient phosphorescence, all singlet and triplet excitons are

harvested in the compounds' lowest triplet states.[2-5,8,9,11,12,14,20-28] This mechanism is denoted as *triplet harvesting mechanism*.[2-5,8,9,11,18,27,28] (ii) An alternative exciton harvesting mechanism[29] is based, for example, on Cu(I), Ag(I), W(VI), Au(III) and Au(I) complexes[1,10,16,27,30-78] or specifically designed purely organic molecules[79-89] that show the molecular effect of thermally activated delayed fluorescence (TADF).[90] In an OLED emission layer, these materials can harvest all excitons in the lowest singlet and triplet states. For most compounds, the phosphorescence from the triplet state T_1 to the electronic ground state S_0 is largely forbidden. However, if the energy separation between the T_1 state and the next higher lying singlet state S_1 is small enough, for example, displaying $\Delta E(S_1\text{-}T_1) < 1000\ cm^{-1}$ (125 meV)[49] thermal activation from T_1 to the S_1 state can be efficient at ambient temperature. Hence, all excitons can be converted into light via emission from the singlet state. Therefore, this mechanism has been denoted as *TADF-singlet harvesting mechanism*. (iii) Recently, another mechanism has been proposed[91-93] by which particularly short emission decay times could be achieved. This was realized by application of specifically developed organic molecules that exhibit an almost ignorable energy separation $\Delta E(S_1\text{-}T_1)$ compared to the energy available at ambient temperature of 210 cm^{-1} (26 meV). Moreover, appropriate electronic structure design was required to guarantee fast intersystem crossing (ISC) between the S_1 and T_1 states. Accordingly, also by this mechanism all singlet and triplet excitons can be converted into light. Due to the very small energy separation and the *direct* and fast equilibration between singlet and triplet states without time-delaying TADF processes, this mechanism has been denoted as *direct singlet harvesting (DSH) mechanism*.[91-93] (iv) Very recently, the *doublet harvesting mechanism* was proposed. Applying this mechanism, also 100% of the excitons can be transferred into light, particularly, for deep blue light generation in combination with hyper-fluorescence for very fast decaying electro-luminescence.[94]

Each of the described exciton harvesting mechanisms requires design of specific emitter materials. Moreover, they have to be optimized, for example, with respect to the emission color, OLED efficiency and performance, emission band width, and especially, short decay time[49,59,62,91,95] to reduce roll-off and device stability problems.[95] Furthermore, environmental compatibility and availability at reasonable costs cannot be disregarded.

In this contribution, we want to focus on environmentally friendly TADF-singlet harvesting Cu(I) and Ag(I) complexes. Although many investigations with such complexes have already been carried out, it is still a challenge to design new materials that exhibit high emission quantum yields at short TADF decay times. This is due to the typical property of Cu(I) or Ag(I) TADF emitters of which the lowest excited states are of metal-to-ligand charge transfer (MLCT) character. Upon excitation of these states, the metal center is formally oxidized. As a consequence, the pseudo-tetrahedral ground state geometry is strongly distorted (flattened) towards a planar geometry.[96-98] In this situation, the Franck-Condon (FC) factors between the low-lying vibrational wavefunctions of the excited states and those of the high-lying vibrations of the electronic ground state become large. This is usually connected with fast non-radiative decay rates and thus, small emission quantum yields.[99] Therefore, it is highly desirable to synthesize rigid complexes with little freedom for distortions in the excited states. For example, use of rigid chelate ligands combined with sterical hindrances between them seems to be an adequate strategy. This approach was already successful for a few Cu(I)[54,58] and Ag(I)[62,100] complexes. Here, we will investigate Cu(I) and Ag(I) complexes with a new rigid tri-dentate N,P,P-ligand, namely 3,5-dimethyl-1-(2-((2-(di-*o*-tolyl)phosphanyl)(*o*-tolyl)-phosphanyl)phenyl)-1*H*-pyrazole (dmpzpp). (Scheme 1, below) Indeed, the resulting complexes Cu(dmpzpp)Br **7**, Cu(dmpzpp)I **8**, Cu(dmpzpp)SPh **9** (with SPh = thiophenolate), and Ag(dmpzpp)I **10** show high emission quantum yields Φ_{PL} of 70% up to 90% for powder materials. Even in films used as hosts for OLED fabrication, the Φ_{PL} decrease is not as drastic

as frequently found. For example, for compound **8** used in an OLED emission layer, a quantum yield of Φ_{PL} = 63% has been determined. Furthermore, these neutral complexes are, at least in part, stable and sublimable without thermal decomposition. Hence, using compounds **8** and **9**, vacuum deposited OLEDs can be fabricated. (See below.)

In the subsequent sections, we first discuss syntheses of the ligand and the complexes and characterize the new materials chemically as well as by X-ray structure determinations. In the next section, we present DFT and TD-DFT computational studies to obtain first insight into the electronic structures of the complexes. Then, we will show that the four compounds studied are TADF emitters. For a representative example, Cu(dmpzpp)SPh **9**, the TADF and phosphorescence behavior will be photophysically discussed in detail. Thereafter, we will present results of vacuum deposited OLEDs using compounds **8** and **9**. Interestingly, the external quantum efficiency (EQE) of the vacuum deposited device with **8** is as high as 16.4%, although the Φ_{PL} value in the applied host film amounts only to 63%. Thus, the EQE value observed is remarkably high. Finally, in a conclusion, strategies for material improvements will be addressed.

Syntheses and characterizations

The new ligand dmpzpp **5** was synthesised in four steps. (2-Bromophenyl)di-*o*-tolylphosphane **1** and chloro-*N*,*N*-diethyl-*o*-tolylphosphanamine **2** were prepared as described in the literature.[101,102] Key intermediate chloro(2-(di-*o*-tolylphosphanyl)phenyl)(*o*-tolyl)phosphane **3** was synthesized in a one-pot-reaction following the sequence of a bromine-lithium exchange at **1**, phosphanylation by amino group protected synthon **2**, finally deprotecting the intermediate with HCl in dioxane. By this protocol chloro functionalized phosphorus electrophile **3** could be isolated as colourless solid in 99% yield! **3** was then converted with 2-(3,5-dimethyl-1*H*-pyrazol-1-yl)phenyl)lithium, generated in situ via an ortho-directed lithiation to give the dmpzpp ligand **5** as colourless powder in 69% yield.

Please print this Scheme over the width of two columns.

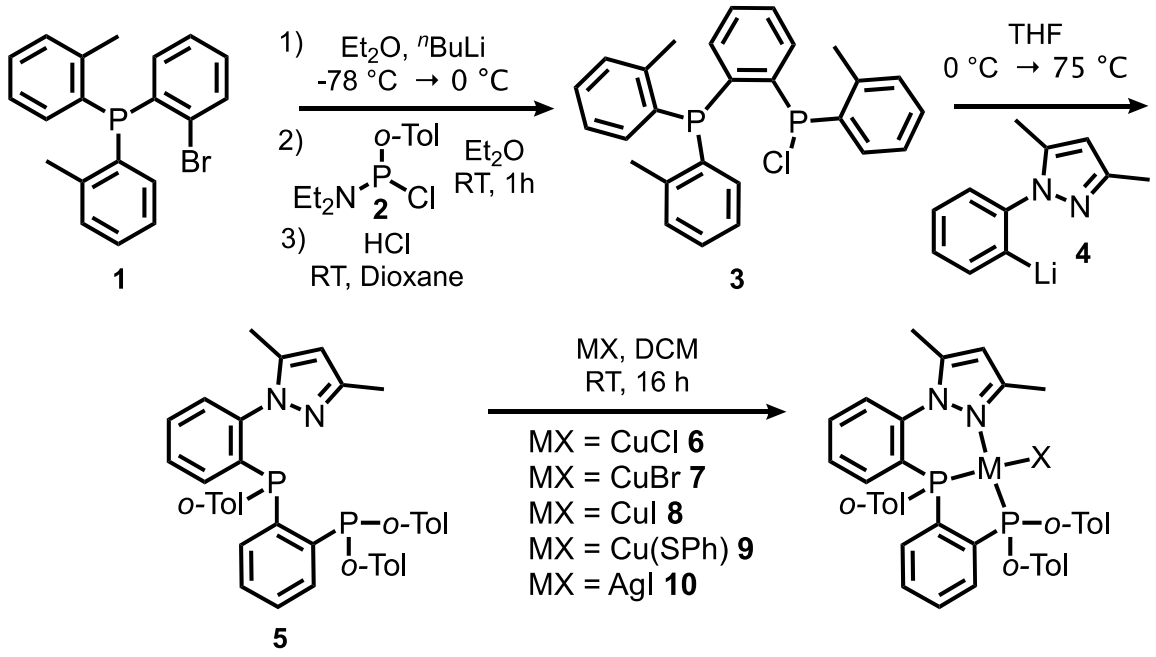

Scheme 1. Synthesis of 3,5-dimethyl-1-(2-((2-(di-*o*-tolyl)phosphanyl)(*o*-tolyl)-phosphanyl) phenyl)-1*H*-pyrazole (dmpzpp **5**) and of highly emissive Cu(dmpzpp)X **6-9** and Ag (dmpzpp)I **10** complexes. The complexes **7** to **10** are characterized below with respect to their emission properties.

In order to synthesize the compounds **6-10**, ligand **5** was dissolved in acetonitrile and reacted with a copper(I) halide (CuCl, CuBr, and CuI), with AgI or with preformed Cu(SPh) at ambient temperature in dichloromethane (DCM). The precipitates formed were collected by centrifugation, washed and dried in vacuum at 60 °C to obtain the desired products **6-9** and **10** as yellow and colorless powders, respectively. (For details see SI-2.) Interestingly, complex **8** can be sublimed at $8.6 \cdot 10^{-7}$ mbar at a temperature of 240-250 °C. The sublimate shows exactly the same NMR spectra as the starting material (see Figure S-14). Thus, this complex is privileged for vacuum processing of an OLED. Compound **9** can also be vacuum processed though at about two orders of magnitude lower vacuum pressure than necessary for **8**. Moreover, all compounds are solution processable without showing high air sensitivity.

Single crystals of the complexes **6-10** could be obtained by layering the corresponding chloroform or acetonitrile solution with *n*-pentane. The complexes crystallize either in a monoclinic (**6**,**7**) or triclinic (**8-10**) crystal system. Single crystal structures of all dmpzpp Cu(I) and Ag(I) complexes were determined by X-ray diffraction analyses. Selected bond distances and angles for **6-10** are listed in Table 1. The crystallographic data and structure refinement details can be found in the supporting information (see SI-5). As representative examples, the molecular structures of **8** and **9** are displayed in Figure 1, the others are described in the supplement (SI-5).

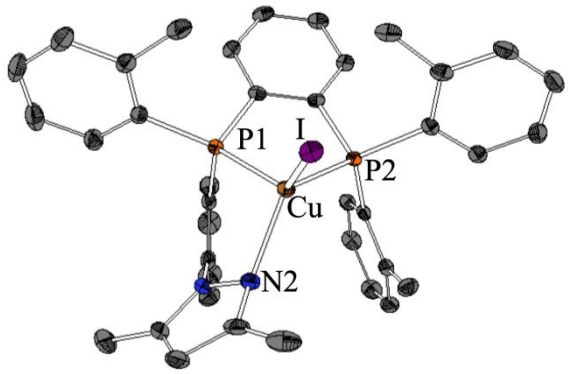

a

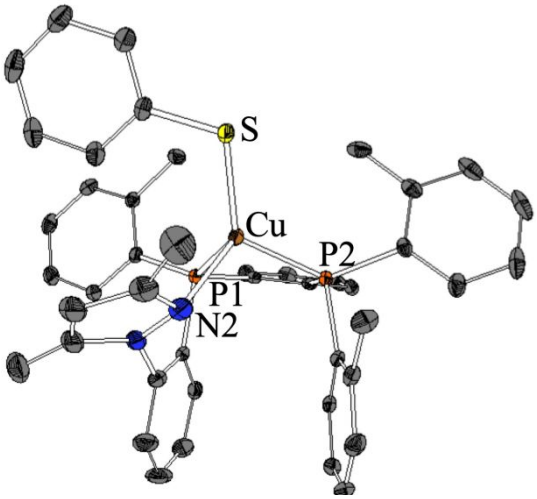

b

Figure 1. Molecular structures of (a) Cu(dmpzpp)I **8** and (b) Cu(dmpzpp)(SPh) **9** from X-ray structure determinations (thermal ellipsoids with 50% probability). Hydrogen atoms and solvent molecules are omitted for clarity.

Table 1. Selected bond distances [Å] and angles [°] based on X-ray diffraction measurements.

Compound	Cu(dmpzpp)Cl **6**	Cu(dmpzpp)Br **7**	Cu(dmpzpp)I **8**	Cu(dmpzpp)(SPh) **9**	Ag(dmpzpp)I **10**
M-P1[a] [Å]	2.2829(7)	2.2508(7)	2.2828(5)	2.2757(4)	2.533(5)
M-P2 [Å]	2.2600(7)	2.2893(7)	2.2756(5)	2.2753(4)	2.488(5)
M-N2 [Å]	2.139(2)	2.148(2)	2.0951(15)	2.2708(16)	2.570(5)
M-X[b] [Å]	2.2674(7)	2.3992(4)	2.5684(2)	2.2403(4)	2.702(6)
P1-M-X [°]	122.45(3)	120.90(2)	123.965(14)	127.314(16)	134.0(3)
P2-M-X [°]	125.26(3)	123.79(2)	115.152(14)	124.065(16)	124.33(16)
N2-M-X [°]	105.50(6)	111.90(6)	112.23(4)	110.22(4)	110.7(2)
P1-M-P2 [°]	87.65(3)	87.66(2)	87.009(17)	87.125(15)	80.83(16)
P1-M-N2 [°]	96.87(6)	93.65(6)	95.81(4)	91.98(4)	84.18(14)
P2-M-N2 [°]	115.59(6)	113.18(6)	119.77(4)	110.77(4)	115.4(2)

a. M = Cu, Ag;

b. X = Cl, Br, I, SPh.

In all complexes, the central metal ion shows a pseudo-tetrahedral configuration, where the P-M-X angles are with 115.152(14)° to 134.0(3)° significantly larger than for an ideal tetrahedron with 109.5°. Therefore, the P1-M-P2 and P1-M-N2 angles with 80.83(16)° to 96.87(6)° are smaller, while the N2-M-X angles with 105.50(6)° to 112.23(4)° and the P2-M-N2 angles with 110.77(4)° to 119.77(4)° fall partly closer to the ideal tetrahedral angle. As expected, the M-X distances increase within the period of the halides and from cupper(I) to silver(I) with the effective ionic radii.[103] The significantly shorter Cu-S distance in the thiophenolato complex **9** is an indicator for the thiophilicity of copper(I), a consequence of a soft acid-base interaction according to Pearson[104] and is even shorter (2.2403(4) Å) than the Cu-S distance in a comparable complex [$(Ph_3P)_2$(py)CuSH] (2.322(1) Å (py = pyridine).[105] The Cu-P distances are between 2.2508(7) Å and 2.2829(7) Å being consistent with the ones reported for

$[(Ph_3P)_2(py)CuX]$ with X = Cl, Br, I.[106] The Ag-P distances amount to 2.533(5) Å and 2.488(5) Å for complex **10** and are marginally shorter than the Ag-P distances in $[(Ph_3P)_3AgI]$.[107]

Electronic structures. DFT and TD-DFT computations

Computational studies (PBE-D3(BJ)/def2-TZVPP) were performed on the model compounds Cu(dmpzpp)I **8** and Cu(dmpzpp)(SPh) **9** to obtain first insights into the electronic structures. Taking into account that the lowest excited states S_1 and T_1 essentially determine the luminescence properties of the complexes, the contribution of the HOMO → LUMO transition was studied. For **8,** this excitation contributes with 99.9% to the S_1 state and with 98.9% to the T_1 state as calculated for the vertical excitation for the optimized T_1 state geometry. For **9**, the values are 99.8% and 99.9%, respectively. The Kohn-Sham orbitals of HOMO and LUMO, as displayed in Figure 2, show only small overlap. This means that the S_1 and T_1 states are of distinct charge transfer character and it implies relatively small $\Delta E(S_1\text{-}T_1)$ values and small transition dipole moments.[38,49] For Cu(dmpzpp)I **8**, the HOMO is mainly Cu (6.1% $d_{x^2-y^2}$, 3.1% d_{yz}, 2.8% d_{xz}) and I based and the LUMO is essentially located on the phenyl backbone of the 2-(3,5-dimethyl-1*H*-pyrazol-1-yl)phenyl fragment. The HOMO of Cu(dmpzpp)(SPh) **9** is delocalized over Cu (6.1% $d_{x^2-y^2}$, 5.8% d_{yz}) and the thiophenolate (S: 18.5% p_z, 10.2% p_x, Ph: 15.8% p (sum of p-orbitals of the aromatic C atoms)) ligand and the LUMO of **9** is similar to the one of **8**. For simplicity, we denote the corresponding transitions as metal-to-ligand charge transfer (MLCT) transitions. Although the calculated transition energies are too small, if compared to the experimental ones, we assume that the energy differences display the experimental situation more realistically. Thus, for **8** and **9** we find $\Delta E(S_1\text{-}T_1)$ = 774 cm^{-1} (96 meV) and 319 cm^{-1} (40 meV), respectively, if we refer to the T_1 state optimized geometries. (Tables S-7 and S-14) The experimental energy gap, only determined for compound **9**, amounts

to 600 cm^{-1} (74 meV). (Figure 5, below) These energy separations are sufficiently small, to predict an occurrence of efficient TADF for these complexes.

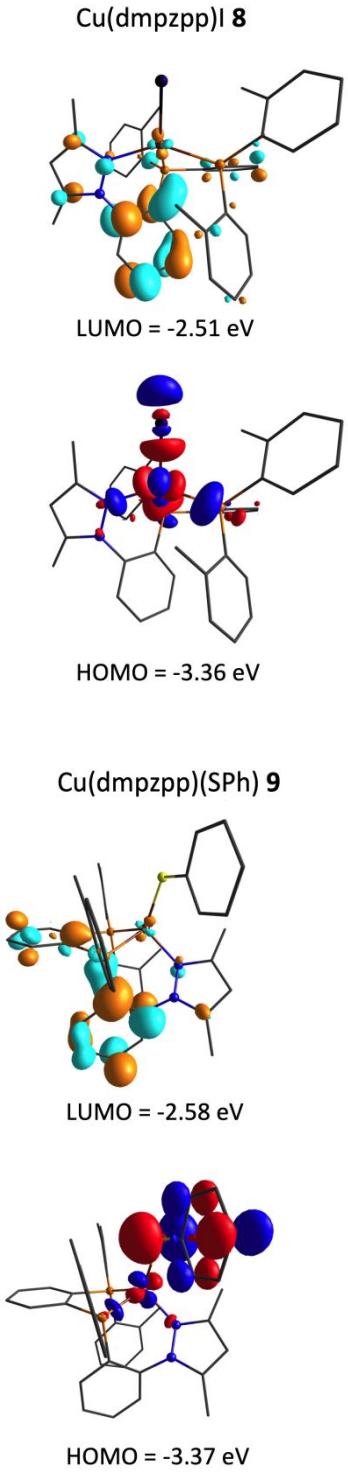

Figure 2. Kohn-Sham orbitals of Cu(dmpzpp)I **8** and Cu(dmpzpp)SPh **9** calculated for the optimized T_1 state geometry (iso-value = 0.05). Calculations were performed at the PBE-D3(BJ)/def2-TZVPP level of theory. The orbitals shown largely correspond to the NTOs

(natural transition orbitals) of both the T_1 and S_1 states of **8** and **9**, respectively. Thus, HOMO and LUMO match to hole and electron, respectively.

Furthermore, we calculated the geometries of the electronic ground state S_0, the first exited singlet S_1 and the first excited triplet state T_1 of Cu(dmpzpp)I **8** and Cu(dmpzpp)(SPh) **9**. As expected, the S_0 molecular geometries of **8** and **9** are found to be in reasonable agreement with the geometries obtained from single crystal X-ray diffraction analyses (see SI Tables S-6 and S-13). Usually, for Cu(I) and Ag(I) complexes geometry rearrangements will occur upon excitation. Indeed, when comparing the ground state S_0 geometries with those of the excited states S_1 and T_1, structural rearrangements are displayed by the calculations, being more distinct for the $S_0 \rightarrow T_1$ than for the $S_0 \rightarrow S_1$ transition. (Tables S-6, S-13, Figures S-20, and S-24) For **8**, the structural rearrangements in the excited state are significantly larger than for **9**. For compound **8**, the I-Cu-P1 angle changes from 121.6° in the S_0 state to 159.0° in the T_1 state or to 125.9° in the S_1 state, which is notably less compared to the T_1 state. Changes of the I-Cu-P2 and I-Cu-N angles are also significant, amounting to 122.8° (S_0)/99.4° (T_1) and to 111.0° (S_0)/106.7° (T_1), respectively, while the deformation in the S_1 state is almost negligible 122.8° (S_0)/122.7° (S_1) and 111.0° (S_0)/111.2° (S_1), respectively. For compound **9,** the structural rearrangements are significantly less pronounced, since for this complex, the halide is replaced by the more bulky thiophenolate ligand. The S-Cu-P1 angle changes only from 122.1° (S_0) to 113.2° (T_1) or to 120.1° (S_1), while the angles S-Cu-P2 vary from 123.3° (S_0) to 121.4° (T_1) or 120.3° (S_1) and S-Cu-N from 111.7° (S_0) to 117.0° (T_1) or to 115.7 (S_1). Figure 3 summarizes the geometries in the different states for Cu(dmpzpp)(SPh) **9** to visualize the small geometry changes for the complex with the bulky ligand. From these theoretical predictions, it is expected that the more bulky compound Cu(dmpzpp)(SPh) **9** shows a higher emission quantum yield than Cu(dmpzpp)I **8**. This is consistent with experimental observations (see below).

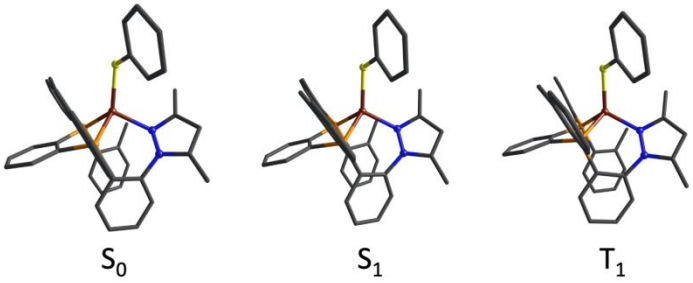

Figure 3. Optimized geometry of Cu(dmpzpp)(SPh) **9** for the S_0, S_1, and T_1 states in gas phase. The diagram illustrates that only small distortions occur upon excitation due to the bulky ligands in **9**. Calculations were performed at the PBE-D3(BJ)/def2-TZVPP level of theory. Hydrogen atoms are omitted for clarity.

TADF properties

DFT and TD-DFT calculations show that the lowest excited states are of ^{1}MLCT (S_1) and ^{3}MLCT (T_1) character, respectively. For the discussed compounds **8** and **9**, these states stem to more than 98% from HOMO → LUMO excitations. These orbitals are essentially localized in the metal-halide or metal-thiophenolato molecular range (HOMO) and on the N,P,P ligand (LUMO), respectively. (Figure 2) Accordingly, a relatively small exchange interaction between the unpaired electrons occurs, giving $\Delta E(S_1\text{-}T_1)$ values of several hundred cm^{-1}. Hence, TADF is expected to be found at ambient temperature. Indeed, already simple spectroscopic studies at 300 K and at 77 K can demonstrate this property.[37,38,49] (Table 2) At low temperature, the compounds exhibit a long-lived $T_1 \rightarrow S_1$ phosphorescence (slow radiative rate). With increasing temperature, the energetically higher lying S_1 state is successively populated opening the additional radiative TADF deactivation path, which leads to a dramatic decrease of the emission decay time or to a drastic increase of the radiative rate. This is particularly distinct, if the 77 K and 300 K decay times of compound **7** are compared, showing a decrease by a factor of more than 360. In parallel, the emission spectra exhibit a slight blue shift (if not hidden in the broad emission bands) due to the higher energy of the S_1 state compared to the T_1 state. (Table 2)

Table 2. Emission data measured for powders. λ(max), τ, and Φ_{PL} represent the wavelength of the emission peak maxima, the emission decay time, and the emission quantum efficiency, respectively.

Compound	T/K	λ(max)/nm	τ/μs	Φ_{PL}/%	k^r /s^{-1} [a]
7	300	541	9	83	$9.2 \cdot 10^4$ s^{-1}
Cu(dmpzpp)Br	77	551	3300	85[b]	$2.6 \cdot 10^2$ s^{-1}
8	300	530	7	82	$12 \cdot 10^4$ s^{-1}
Cu(dmpzpp)I	77	530	≈ 420	85[b]	$20 \cdot 10^2$ s^{-1}
9	300	540	5	90	$18 \cdot 10^4$ s^{-1}
Cu(dmpzpp)SPh	77	540	680	70	$10 \cdot 10^2$ s^{-1}
10	300	479	13	70	$5.4 \cdot 10^4$ s^{-1}
Ag(dmpzpp)I	77	484	270/470[c]	-	-

a. Radiative rate calculated according to $k^r = \Phi_{PL}/\tau$
b. Estimated value, absolute error ± 15%
c. Bi-exponential decay.

Although Cu(I) complexes mostly show TADF behavior,[1,37,38,49] for Ag(I) complexes, TADF is relatively rare.[48,62,63,64,108,109] This is related to the differences of the oxidation potentials of the 3d/4d-electrons. For Ag^+ it is significantly higher than for Cu^+.[110] Thus, frequently, the 4d-orbitals of Ag^+ complexes are energetically even lower than the occupied orbitals of the organic ligands. Hence, the lowest excited states of the complexes are not of MLCT but of ligand-centered (LC) character and thus, usually show long-lived phosphorescence even at ambient temperature, but no TADF.[100,111-114] Therefore, the design of Ag(I) complexes that exhibit short-lived TADF requires attention with respect to the choice of the organic ligands. They should induce an energy destabilization of the deep-lying 4d-orbitals. This can be achieved by ligands with good electron donating properties, such as ligands with phosphine coordination to the metal center. Indeed, this is realized in compound **10**. Due to the energy destabilization of the d-orbitals they strongly contribute to the HOMO. As a consequence, TADF emission is observed. Interestingly, as a net result, the transition energy is usually higher than for the related Cu(I) complex with the same ligands. In fact, these properties are displayed in Table 2.

Ag(dmpzpp)I **10** shows blue TADF at λ_{max}= 479 nm, while Cu(dmpzpp)I **8** exhibits green emission at 530 nm.

Simple considerations allow us also to qualitatively understand the blue shift of the TADF emission of Cu(dmpzpp)Br **7** with λ_{max}= 541 nm to Cu(dmpzpp)I **8** emitting at λ_{max}= 530 nm. This shift can be rationalized by a decrease of the ligand field strength from Br to I.[115] Accordingly, the resulting smaller splitting of the 3d-orbitals, being involved in the HOMO, leads to an energy stabilization of the highest-lying 3d-orbital of the iodido complex compared to the bromido complex, while the LUMO remains almost un-shifted. As a consequence, higher emission energy occurs for compound **8** than for compound **7**. (Table 2) This trend is similarly displayed by our TD-DFT computations. (Tables S-4 and S-11) Equivalent behavior has also been described for other Cu(I) complexes.[40,52]

In conclusion, all compounds studied exhibit relatively short-lived and efficient TADF at ambient temperature with high emission quantum yields at radiative TADF decay rates between $5 \cdot 10^4\,s^{-1}$ and $18 \cdot 10^4\,s^{-1}$. At T = 77 K, one observes only long-lived phosphorescence with around two orders of magnitude slower decay rates. The emission colors are green to yellow for the copper complexes and blue for the silver compound.

In the subsequent section, we will present a detailed discussion of phosphorescence and TADF properties by studying the representative compound Cu(dmpzpp)SPh **9** over the large temperature range from T = 1.7 K to 300 K.

Detailed analysis of phosphorescence and TADF properties of Cu(dmpzpp)SPh 9

From the series of compounds studied in this contribution, we select Cu(dmpzpp)SPh **9** for more detailed investigations. It exhibits the highest emission quantum yield of this series of Φ_{PL} = 90%. This is due to the bulky coordination around Cu and the fast (radiative) TADF decay

rate of $k^r(TADF) = 18 \cdot 10^4\ s^{-1}$ ($\tau^r = 5.6\ \mu s$). This rate is also relatively fast if compared to other Cu(I) complexes.[37,38,49]

Spectra and quantum yields

Figure 4 reproduces absorption and emission spectra of Cu(dmpzpp)SPh **9** recorded in various environments. The absorption is measured in dichloromethane (DCM). The different bands recognized in the range of 230 to 350 nm are assigned to ligand centered $\pi\pi^*$ transitions, while the weaker absorptions from about 350 to 450 nm are characterized as MLCT transitions (compare the computational studies discussed above).

The emission spectra are found with significant Stokes shift. They are very broad as expected for charge transfer (CT) transitions. At ambient temperature, one essentially observes TADF from the S_1 (^{1}MLCT) state peaking at 540 nm (yellow). The TADF quantum yield of the powder material is with $\Phi_{PL} = 90\%$ very high. Upon cooling to T = 77 K, TADF is frozen out and one finds the $T_1(^3MLCT) \rightarrow S_0$ phosphorescence. The quantum yield drops to $\Phi_{PL} = 70\%$. Such a behavior is not frequently observed, but compare[62]. It can be rationalized by the drastic decrease of the radiative rate from $k^r(TADF) = 18 \cdot 10^4\ s^{-1}$ (300 K) to $k^r(phos) = 10 \cdot 10^2\ s^{-1}$ (77 K) by more than two orders of magnitude. (Table 2) Using the relation for the non-radiative rate $k^{nr} = (1 - \Phi_{PL})/\tau$, $k^{nr}(phos) = 4.4 \cdot 10^2\ s^{-1}$ (77 K) is obtained. Thus at T = 77 K, the non-radiative processes can moderately compete with the radiative one. On the other hand, at T = 300 K with $k^{nr}(TADF) = 2 \cdot 10^4\ s^{-1}$ (300 K) the radiative rate strongly prevails the non-radiative one.

With temperature decrease from T = 300 K to 77 or to 50 K, when TADF is frozen out, one would expect a small red shift due to the $\Delta E(S_1\text{-}T_1)$ energy gap. However, if the gap is relatively small (for **9**: 600 cm^{-1}, 74 meV, see below), the shift may be hidden by the broad band emission. Such a behavior has also been observed for other TADT Cu(I) complexes.[52,55]

The emission of compound **9** in less rigid environments than in crystalline powders shows significant reduction of the quantum yield. For the compound doped in relatively soft PMMA (poly(methyl methacrylate)) and dissolved in fluid DCM, respectively, Φ_{PL} values of 56% and only ≈ 1% are observed. (Table 3, below) This Φ_{PL} reduction is explained by the more distinct geometry changes upon excitation in the softer environment. As a consequence, the non-radiative deactivation processes can become more pronounced due to the higher FC factors of the excited and ground state vibrational wavefunctions. Thus, the quantum yield drops as compared to a more rigid environment. Moreover, the geometry change usually results in a red shift of the emission spectra with respect to the more rigid crystalline environment. Indeed, a red shift of ≈ 4 nm is found for the peak maxima. (Figure 4)

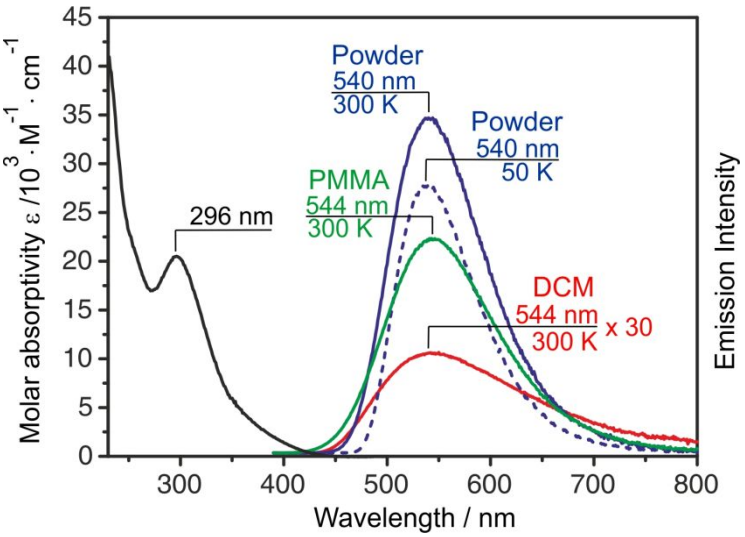

Figure 4. Absorption and emission spectra of Cu(dmpzpp)SPh **9**. Absorption spectrum (black line) recorded in dichloromethane (DCM) solution (concentration c ≈ 10^{-5} M) at 300 K, emission spectra as powder (blue lines), doped in PMMA (green line, c ≈ 1 w%), and dissolved in DCM solution (red line, c ≈ 10^{-5} M). The emission intensity of the solution spectrum is displayed 30 times enlarged. λ_{exc} = 330 nm.

For completeness, we want to point out that an occurrence of a geometry distortion has an important consequence.[11,30,38,58] Typically, it is not possible to conclude on emission properties of individual molecules from investigations of neat materials (powders), because inter-

molecular effects, such as resonant energy transfer to neighboring molecules and finally to quenching impurities, will usually at least influence the emission decay behavior or quantum yield and frequently even quench the emission totally (concentration quenching). However, for most Cu(I) complexes, the geometry distortions upon excitation are strong enough, even in the neat powder phase, to lower the excited states energies sufficiently, so that resonant energy transfer to adjacent non-excited molecules is largely prevented. Accordingly, the excitation is trapped at the initially excited molecule. Such a self-trapping effect[116,117] is the basis for the studies presented in this contribution.

The explanation given above is nicely supported by a recent investigation with Cu(I) tripod complexes with a specifically designed rigid and bulky ligand coordination, in particular, [Cu(tpym)(P(*o*-butyl-ph)$_3$)]PF_6, wherein tpym represents tris(2-pyridyl)methane and P(*o*-butyl-ph)$_3$ tris(*ortho*-n-butylphenyl)phosphine.[58] Accordingly, geometry distortions in the excited state are largely prevented. As a consequence, a TADF material was developed that shows the highest emission quantum yield in fluid solution reported so far (86%).[58] Interestingly, the corresponding powder material displays a significantly smaller quantum yield (56%). Obviously, the self-trapping effect is partly suppressed in the rigidified molecule. Thus, concentration quenching can occur, in contrast to the situation found for almost all other Cu(I) complexes.

In conclusion, the emission measured at ambient and lower temperature, even if cooled to T = 1.7 K (not reproduced), show only broad bands. Accordingly, investigation of such spectra does not disclose detailed information of the compound's photophysical properties. However, from studies of the emission decay behavior, we know from the data presented in Table 2 that significant changes occur with temperature change. Therefore, in the subsequent section, we will study the decay behavior. Indeed, it will be shown that a deeper insight in the electronic structure and radiative relaxation properties thus becomes possible.

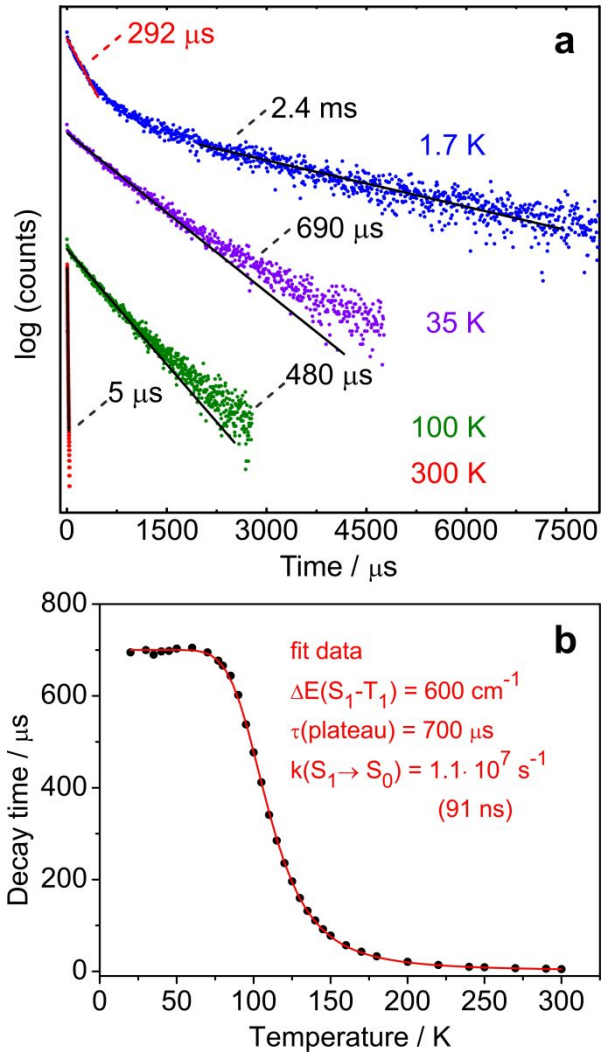

Figure 5. Emission decay behavior of Cu(dmpzpp)SPh **9** powder. (a) reproduces emission decay curves measured at selected temperatures. Approximated decay components (fits) are inserted. (b) shows the emission decay time versus temperature (black dots) and the fit according to eq. (1) (red line). λ_{exc} = 378 nm, excitation pulse width < 100 ps, λ_{det} = 530 nm.

Emission decay, energy levels, and transition rates

Figure 5a reproduces decay curves for several selected temperatures. Apart from the 1.7 K decay that follows nearly bi-exponential decay dynamics (for details see below), we can approximate the decay at higher temperature mono-exponentially. Such a behavior corresponds to fast equilibration between the involved emitting states, i.e. faster than the decays of the

individual states, and it excludes extensive inhomogeneity effects within the ensemble of emitting complexes (but compare ref.[118]). In this situation, we can apply a Boltzmann-type equation to characterize the temperature dependence of the emission decay time τ(T) according to[1,11,49,119]

$$\tau(T) = \frac{3 + \exp\left(-\frac{\Delta E(S_1 - T_1)}{k_B T}\right)}{3k(T_1) + k(S_1)\exp\left(-\frac{\Delta E(S_1 - T_1)}{k_B T}\right)} \quad (1)$$

Herein, $\Delta E(S_1\text{-}T_1)$ refers to the energy separation between the S_1 and T_1 states. $k(S_1)$ and $k(T_1)$ are the rates of the $S_1 \rightarrow S_0$ and $T_1 \rightarrow S_0$ transition, respectively. k_B is the Boltzmann constant. If we assume coarsely constant rates and quantum yields over the whole temperature range, fitting of eq. (1) to the experimental data given in Figure 5b leads to a well matching fit curve. This dependence displays nicely the changes of the emission processes within the temperature range studied. At low temperature between $20 \leq T \leq 70$ K, one observes a plateau showing the decay time of $\tau(phos) = 700$ μs, displaying the phosphorescence of compound **9**. It corresponds to the radiative decay time of $\tau^r(phos) = \tau(phos)/\Phi_{PL} = 1$ms. Above T = 70 K, the decay time sharply decreases and finally reaches a value of 5 μs at ambient temperature. The decrease is induced by thermal population of the higher lying S_1 state and by the fact that the spin-allowed $S_1 \rightarrow S_0$ fluorescence is drastically faster than the spin-forbidden $T_1 \rightarrow S_0$ phosphorescence, leading to the TADF effect.

For completeness, it is remarked that a prompt $S_1 \rightarrow S_0$ fluorescence with a decay time of 91 ns (Figure 5b and below) is not observed with our experimental time resolution, because the competing $S_1 \rightarrow T_1$ ISC process, occurring in about 30 ps[120], is by more than three orders of magnitude faster.

Using the fit procedure according to eq (1), we obtain the energy gap of $\Delta E(S_1\text{-}T_1) = 600\ cm^{-1}$ (74 meV) and the rate for the $S_1 \rightarrow S_0$ transition of $k(S_1) = 1.1 \cdot 10^7\ s^{-1}$ (91 ns). (Figures 5 and 6, Table 3) Both parameters are of dominating importance for the TADF decay time at ambient temperature. The resulting value of τ(TADF) = 5 µs or of τ^r(TADF) = 5.6 µs is relatively short if compared to conventional TADF emitters. Usually, short decay times are required for obtaining long-lived OLED devices.[1,95]

Table 3. Photophysical data of Cu(dmpzpp)SPh **9** as powder, doped in PMMA (≈ 1 w%), and in fluid dichloromethane (DCM) solution (c ≈ 10^{-5} M).

	powder	PMMA	DCM
λ_{max} (300 K)	540 nm	544 nm	544 nm
Φ_{PL} (300 K)	90%	56%	1%
τ(300 K)	5 µs	7 µs	4 µs
k^r(300 K)	$18 \cdot 10^4\ s^{-1}$	$8.0 \cdot 10^4\ s^{-1}$	$0.25 \cdot 10^4\ s^{-1}$
k^{nr}(300 K)[a]	$2.0 \cdot 10^4\ s^{-1}$	$6.3 \cdot 10^4\ s^{-1}$	$25 \cdot 10^4\ s^{-1}$
λ_{max} (50 K)	540 nm		
Φ_{PL} (77 K)	70%		
$\tau(T_1$, 50 K) plateau	700 µs		
$k^r(T_1$,50 K)[b]	$10 \cdot 10^2\ s^{-1}$		
$k^{nr}(T_1$,50 K)[a, b]	$4.3 \cdot 10^2\ s^{-1}$		
$k^r(S_1 \rightarrow S_0)$[c]	$1.1 \cdot 10^7\ s^{-1}$ (91 ns)		
$\Delta E(S_1 - T_1)$[c]	600 cm^{-1}		
τ(I), τ(II), τ(III)[d]	2.4 ms, 2.25 ms, 292 µs		

a. Non-radiative rate calculated from $k^{nr} = (1\text{-}\Phi_{PL})/\tau$
b. It is assumed that $\Phi_{PL}(50\ K) \approx \Phi_{PL}(77\ K)$
c. From a fit of the τ(T) plot (Figure 5b) using eq. (1)
d. Individual decay times of the three triplet substates, determined at T = 1.7 K

The decay behavior at very low temperature, at T = 1.7 K for example, is distinctly non-mono-exponential. This is a consequence of slow thermalization between the three T_1 substates I, II, and III according to slow rates of spin-lattice relaxation (SLR) at low temperature, if the zero-field splitting ΔE(ZFS) between these states is small, e. g. less than a few cm^{-1}.[121] In this situation, the individual triplet substates emit independently with their intrinsic decay times τ(I), τ(II), and τ(III). From the decay curve measured at T = 1.7 K, we identify two decay components of 292 μs and 2400 μs, but the third one is hidden. (Figure 5a) However, at higher temperature, at 10 or 20 K for example, SLR rates become fast[121] and an average decay time τ_{av} of the three substates is obtained, which can be expressed by[121,122,123]

$$\tau_{av}(T_1\text{-}S_0) = 3(\tau(I)^{-1} + \tau(II)^{-1} + \tau(III)^{-1})^{-1} \quad (2)$$

Using this equation, we can estimate the hidden component. If τ_{av} is given by the experimental phosphorescence decay time of 700 μs (plateau) and two substate decay components are the ones displayed in Figure 5a in the T = 1.7 K decay, we can estimate the hidden component to ≈ 2.25 ms. This value is not very different from the longer-lived component used for this estimate. Two long-lived and similar decay components have also been reported for other Cu(I) compounds.[30,38,49,52] To summarize, the individual decay times of the substates of compound **9** are τ(I) = 2.4 ms, τ(II) = 2.25 ms, and τ(III) = 292 μs without having the information on the energetic order of the three substates. Table 3 and Figure 6 summarize the emission data worked out for Cu(dmpzpp)SPh **9**.

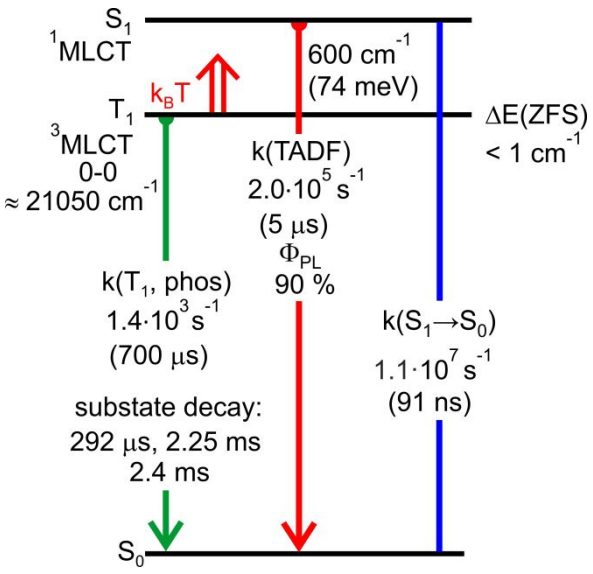

Figure 6. Simplified energy level diagram and decay data for Cu(dmpzpp)SPh **9** powder. The T_1 state consists of three triplet substates I, II, and III that emit independently at T = 1.7 K with estimated values of τ(I) = 2.4 ms, τ(II) = 2.25 ms, and τ(III) = 292 μs. The 0-0 energy given for the $T_1 \rightarrow S_0$ transition is estimated from the blue energy flank of the phosphorescence band as displayed in Figure 4. The values given for k(T_1, phos) and k(TADF) refer to a representative temperature of the τ(T) plateau (for example T = 50 K) and 300 K, respectively.

From the decay behavior at T = 1.7 K, we can conclude[121-125] on a ΔE(ZFS) value of < 1 cm^{-1} (0.1 meV), presumably << 1 cm^{-1}.[125] Such a small ZFS combined with the very long phosphorescence decay time of τ(phos) = 700 μs (τ^r(phos) = 1ms) demonstrates[11] very weak spin-orbit coupling (SOC) of higher lying singlets to at least to one of the emitting T_1 substates. This can be understood taking the following quantum mechanical consideration into account: SOC between the S_1 and T_1 states that stem from the same HOMO→LUMO excitation is almost negligible[28,32,38,49] (El-Sayed rule[126]). Among the series of compounds discussed, Cu(dmpzpp)Br **7** displays the El-Sayed forbiddenness particularly clearly: Although, ΔE(S_1-T_1) amounts only to 680 cm^{-1} (84 meV) (Figure S-27) SOC between the S_1 and T_1 states seems to be unimportant, since the phosphorescence decay time τ^r(phos) at the plateau is as long as 4.0 ms. (Figure S-27) Obviously, the El-Sayed rule, originally presented for purely organic

molecules, is also valid for organo-transition metal compounds. On the other hand, efficient SOC requires quantum mechanical admixture(s) with states that result from a different orbital configuration involving a different d-orbital than the one contributing to the HOMO, for example, HOMO-1. According to results from TD-DFT calculations of compound **9**, the next nearest singlet state with a different d-orbital contribution stems from the HOMO-1→LUMO excitation, giving the state S_5. However, the energy separation that would be of crucial importance for quantum mechanical admitures[28,127,128], in this case $\Delta E(S_5\text{-}T_1)$, is as large as 0.89 eV (7180 cm^{-1}). (Table S-17). Usually, at such a big energy separation direct SOC is not efficient.[38] Interestingly, the situation for Cu(dmpzpp)Br **7** and Cu(dmpzpp)I **8** concerning the energy separations to admixing singlet states is similar (Tables S-5, S-10), but for Cu(dmpzpp)Br **7** the phosphorescence decay time is even about five times longer than for **9**. (Table 2) Hence, it is expected that for all three compounds other processes than direct SOC, such as spin-vibronic coupling[129,130,131], have to be considered that open the phosphorescent decay paths. In contrast, the TADF process is based, after thermal activation, on a spin-allowed singlet-singlet emission and thus, is more than two orders of magnitude faster than the phosphorescent decay.

Electroluminescent properties of Cu(dmpzpp)I 8 and Cu(dmpzpp)SPh 9

To evaluate the electroluminescent (EL) properties of neutral and sublimable Cu(I) complexes **8** and **9**, vacuum-deposited OLEDs with the device structure of ITO/HAT-CN(5 nm)/TAPC (40 nm)/TCTA (10 nm)/TCTA: DPEPO: Cu complex (10 nm)/DPEPO (40 nm)/LiF (1.2 nm)/ Al (100 nm) were fabricated and characterized. In these devices, HAT-CN (1,4,5,8,9,11-hexaazatriphenylene hexacarbonitrile) was used as hole-injecting layer (HIL), TAPC (1,1-bis-(4-bis(4-methylphenyl)-amino-phenyl)-cyclohexane) as hole-transporting layer, TCTA (4,4′,4″-tris(*N*-carbazolyl)-triphenylamine) as electron/exciton-blocking layer, and DPEPO (bis[2-(diphenylphosphino)phenyl] ether oxide) as electron-transporting layer. The mixture of

TCTA and DPEPO with a weight ratio of 1:1 was used as the co-host of the emitting layer (EML) to maximize the performances of our Cu(I) complex based OLEDs. The chemical structures of HAT-CN, TAPC, TCTA and DPEPO are shown in the SI (Scheme 1). Compounds **8** and **9**, respectively, were used as the emitting dopants with concentrations of 2, 4, and 8 wt% in the EML.

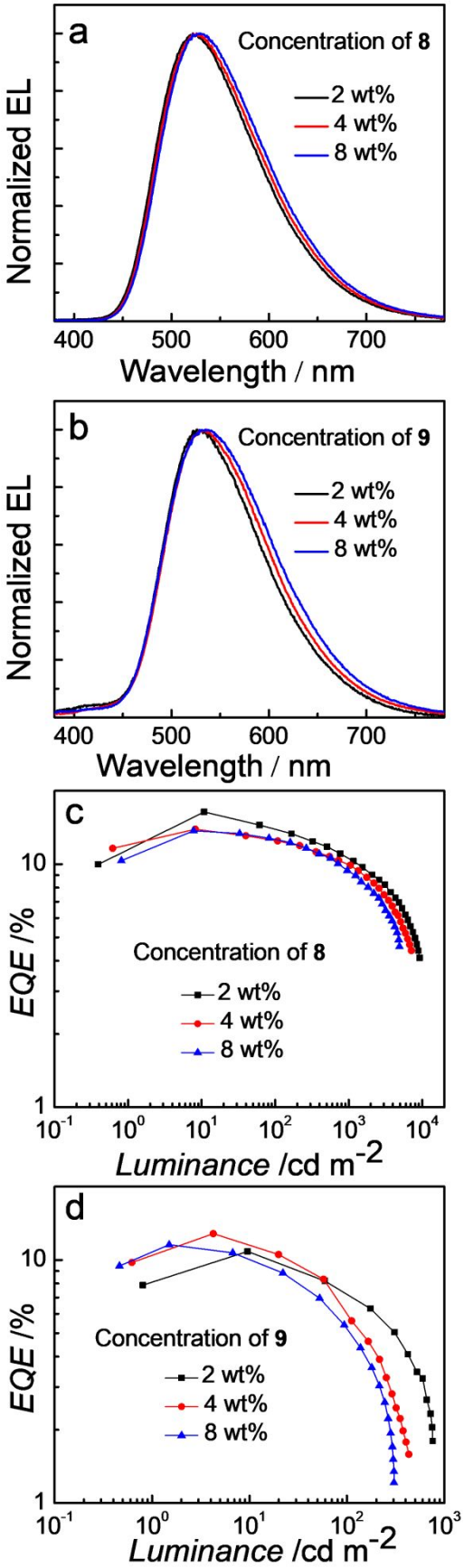
a
Concentration of 8
2 wt%
4 wt%
8 wt%
Normalized EL
400
500
600
700
Wavelength / nm
b
Concentration of 9
2 wt%
4 wt%
8 wt%
Normalized EL
400
500
600
700
Wavelength / nm
c
10
1
EQE /%
Concentration of 8
2 wt%
4 wt%
8 wt%
10^-1
10^0
10^1
10^2
10^3
10^4
Luminance /cd m^-2
d
10
1
EQE /%
Concentration of 9
2 wt%
4 wt%
8 wt%
10^-1
10^0
10^1
10^2
10^3
Luminance /cd m^-2

Figure 7. **a**, **b** Normalized electro-luminescence spectra at 4 V and **c**, **d** external quantum efficiency **(**EQE) *versus* luminance characteristics of vacuum-deposited OLEDs with Cu(dmpzpp)I **8** and Cu(dmpzpp)SPh **9** as emitting dopants with concentrations of 2, 4, and 8 wt%, respectively. Note the different luminance scales of **c** and **d**.

Normalized EL spectra and EQE versus luminance characteristics of these devices are depicted in Figure 7, while the luminance and current density, respectively, versus voltage curves are displayed in the SI (Figures S-28 and S-29). Key performances of these devices are summarized in Table 4. As shown in the Figures 7a and 7b, EL spectra of both compounds **8** and **9** became broader with concentration increase. Similar phenomena were also found in the photo-luminescent (PL) spectra of **8** as depicted in Figure S-30 probably being the result of increasing inhomogeneity of the dopants in the host. Peak maxima of the EL spectra of compounds **8** and **9** are located at around 521 and 535 nm, respectively. This is consistent with the corresponding PL spectra measured in thin TCTA-DPEPO films. Thus, it is concluded that the OLED emission represents TADF of the Cu(I) complex dopants. (The values given for the emission peak maxima slightly deviate from those measured for the powder materials (Table 2) due to the different polarities and rigidities of the emitter's environments.) It is worth to note that the PL spectra of **8** and **9** are quite different. Only one single PL band is seen for compound **8** doped in the TCTA-DPEPO host, while two PL bands are found for the host doped with **9**. (Figure S-30) These bands result from compound **9** and from the host material. Therefore, it is indicated that energy transfer from the host to the Cu(I) compound **9** is inefficient. In fact, a week host emission can also be observed in the EL spectra of the OLED doped with **9**. The host emission decreases with increasing concentration due to more efficient energy transfer. Nevertheless, the relative intensity of the host emission in the EL spectra is much lower than in the PL spectra, indicating that charge-trapping plays an important role in the EL process of the device with **9**. For charge-trapping OLEDs, excitons directly form and recombine on the emitting dopants

without using the step of energy transfer from the electrically excited molecules of the host to the emitter.[132] Compared to the devices based on energy transfer, the current density versus voltage characteristics of charge-trapping devices strongly depend on the dopant concentration because charge-trapping on emitting dopants decreases the charge carrier mobility in the EML.[132,133] As shown in Figure S-29, the decease of current density with increasing concentration at a given driving voltage supports the charge-trapping mechanism of the **9** devices. With the green light emitting OLED based on compound **8** with a doping concentration of 2 wt%, a maximum external quantum efficiency of EQE = 16.4% and a maximum luminance of 9260 cd m^{-2} in the measured voltage range up to 7.5 V at CIE coordinates of (0.33; 0.52) were achieved. (Figure 7 c) If we take into account that the PL quantum yield of compound **8** doped in the TCA-DPEO host amounts only to 63% the EQE value obtained is quite remarkable, because for an extrapolated/assumed value of Φ_{PL}=100%, one could expect to achieve an EQE of 26%. This would be a very high value for a conventional OLED device and thus, shows that the device structure is very well chosen.[1,4,8] Presumably, there is still potential for Φ_{PL} increase by further optimizing the complex' chemical structure (see below). To summarize, the efficiency of this device is among that of the best OLEDs fabricated with Cu(I) compounds by vacuum-deposition technique, so far.[16,31,34,35,39,48,56,60,134-136]

Since the Φ_{PL} value of compound **9** doped in a thin PMMA film with 56% is lower than Φ_{PL} of **8** with 65% in PMMA and since the energy transfer from the host to compound **9** is inefficient, the maximum EQE of device with compound **9** does not reach the value found for the OLED based on compound **8**. It is notable that with increasing luminance, the efficiency roll-off of the device with **9** is significantly more expressed than for the device with **8**. (Figures 7 c and d) Moreover, the maximum luminance obtained for the device with **9** is less than 1000 cd m^{-2}. To find an explanation for these pronounced effects, EL spectra of the device with **9** with 4 wt% dopant concentration were investigated at various driving voltages from 4 to 12 V. (Figure S-

31) With increasing voltage, a new emission band with a maximum at about 565 nm appeared and increased together with an increase of the host emission as shown in Figure S-31b. Accordingly, it is indicated that compound **9** may not be stable when high electric fields are applied and could account for the pronounced efficiency roll-off and the low maximum luminance of OLEDs based on compound **9**. Possibly, the CuS-C bond of the thiophenylate ligand breaks and a stable CuS coordination results. For comparison, as depicted in Figure S-31a, the EL spectra of the device with compound **8** at 4 wt% dopant concentration stayed unchanged with increasing driving voltage. Obviously, the device using Cu(dmpzpp)I **8** is more stable even at a luminance of almost 10000 cd m^{-2}.

Table 4. Key performances of OLEDs with Cu(dmpzpp)I **8** and Cu(dmpzpp)SPh **9** emitters.

Cu(I) complex (concentration)	L_{max} [cd m^{-2}][a]	CE [cd A^{-1}][b]		PE [lm W^{-1}][c]		EQE [%][d]		CIE [(x, y)][e]
		max	at 1000 cd m^{-2}	max	at 1000 cd m^{-2}	max	at 1000 cd m^{-2}	
8 (2 wt%)	9260	41.9	29.1	43.8	21.3	16.4	10.2	0.33, 0.52
8 (4 wt%)	8080	39.5	28.4	41.4	20.3	13.9	9.88	0.35, 0.52
8 (8 wt%)	7600	38.7	26.8	40.5	18.3	13.7	9.38	0.35, 0.52
9 (2 wt%)	760	30.5	N/A	28.2	N/A	10.8	N/A	0.35, 0.51
9 (4 wt%)	433	36.5	N/A	31.8	N/A	12.8	N/A	0.36, 0.52
9 (8 wt%)	304	33.5	N/A	29.2	N/A	11.6	N/A	0.37, 0.52

a. Maximum luminance; b. current efficiency; c. power efficiency; d. external quantum efficiency e. CIE color coordinates at 100 cd m^{-2}.

Conclusion and design considerations for future developments

In this report, we present a new type of Cu(I) and Ag(I) complexes using a rigid tri-dentate N,P,P-ligand, dmpzpp, with the chemical structure shown in Scheme 1. As additional mono-dentate ligand, we apply charged Cl^-, Br^-, I^-, and SPh^-. Hence, the complexes are neutral and sublimable. The powder materials of all complexes exhibit bright TADF of up to 90% photo-

luminescence quantum yield at relatively short emission decay time or fast decay rate at ambient temperature. For example, for Cu(dmpzpp)SPh **9**, the radiative rate amounts to $k^r(TADF) = 1.8 \cdot 10^5\ s^{-1}$ (5.6 µs). (Table 3) This rate is by a factor of almost 200 faster than the phosphorescence radiative rate of $k^r(phos) = 1.0 \cdot 10^3\ s^{-1}$ (1 ms). Accordingly, the TADF process opens a very efficient radiative decay path, which strongly predominates non-radiative quenching. Thus, after freezing out the TADF decay path, for example, by cooling to T = 77 K, Φ_{PL} drops. Therefore, short radiative decay time at ambient temperature is essential for obtaining high emission quantum yields. Maybe, applying a design strategy that leads to an increase of the $S_1 \rightarrow S_0$ transition rate (see eq.(1)), might result in an even further increase of Φ_{PL}. In a recent study with a similar challenge, we could successfully show that such a rate increase was achievable for Ag(I) complexes by changing the relative orientation of HOMO and LUMO.[49,62] This strategy allowed us to distinctly increase the rate $k(S_1\text{-}S_0)$ giving $\Phi_{PL}(TADF) = 100\%$.

The compounds studied cover a large emission color range from yellow to green and to blue for Cu(I) and Ag(I) complexes, respectively, in all cases at high emission quantum yield. Maybe even red emission at high Φ_{PL} might be realizable with this class of compounds. Finding efficient red-light emitters is still a challenge due to quenching processes according to the energy gap law.[99] For our materials, for example, substitution of the N,P,P-ligand with electron-withdrawing groups might lead to such a red shift. This concept, however, is only suitable, if the required fast TADF rate $k^r(TADF)$ can be maintained.

The class of materials studied is attractive for testing OLED properties. In fact, using well sublimable Cu(dmpzpp)I **8**, we find a remarkable OLED performance with an external quantum efficiency of EQE = 16.4%, although compound **8** being doped with 2% in an emission layer (TCTA : DPEPO co-host with a 1 : 1 ratio) exhibits a photo-luminescence quantum yield of only Φ_{PL} = 63%, significantly lower than of the powder material. If we formally assume Φ_{PL} =

100% for the emitter complex in this host, we would expect to find an EQE value of 26%, which demonstrates very good OLED performance. It corresponds to the maximum of out-coupling of light generated by electro-luminescence in conventional OLED device structures, if 100% internal efficiency is obtained.[1-4,9] Obviously, the device structure developed is well suited for compound **8**. Therefore, future developments for increasing EQE should try to design compounds that exhibit almost 100% photo-luminescence quantum yield. However, occurrence of high Φ_{PL} is not only related to the radiative rates as discussed above, but also to non-radiative processes. These are connected to the rigidity of the molecular structure. For example, the structure with bulky ligands strongly reduces distortions that usually occur in Cu(I) or Ag(I) complexes after MLCT excitation. The less distinct such distortions are, the less significant is non-radiative deactivation and the higher is the emission quantum yield.[38,99] However, the extent of the geometry change is usually not only given by the intrinsic molecular rigidity. In most cases, also the environment or the host rigidity is highly important.[38] Even the compound with the most bulky ligand structure studied in this contribution, Cu(dmpzpp)SPh **9**, exhibits a drastic decrease of Φ_{PL} from 90% as rigid powder, to 56% in PMMA, and finally to only 1% in fluid DCM solution. Obviously, this trend indicates that the molecular rigidity of these compounds requires an additional external or matrix-induced component to reach high Φ_{PL} values. However, the host materials usually available for OLED emission layers do not seem to provide sufficient external rigidity. Hence, one is faced with the challenge to design an even more rigid ligand structure. This could already be demonstrated[58], though for a charged and thus, not well sublimable compound. Maybe in future, a rigid tetra-dentate ligand coordination might be realizable. However, if so, it is equally important not to lose TADF efficiency.

In summary, the new compounds presented do not only exhibit attractive TADF properties and OLED performance, they also open promising options for developments of future materials.

Acknowledgements

Financial support by TransMIT - Gesellschaft für Technologietransfer (Gießen,Germany) is gratefully acknowledged.

This work was further supported by Innovation and Technology Fund (PRP/071/19FX), Guangdong Major Project of Basic and Applied Basic Research (2019B030302009), and the Basic Research Program of Shenzhen (JCYJ20170818141858021 and JCYJ20180508162429786).

Associated Content

Supporting Information

The Supporting Information is available free of charge on the ACS Publications website at DOI:…

Syntheses, NMR-Data, sublimation details of **8** and **9**, X-ray crystallography data, quantum chemical calculations, photophysical characterization of **7**, and electro-luminescence properties of OLEDs with 8 and 9 emitters**.** (PDF)

Accession Codes

CCDC 1958853 (**6**), 1958854 (**7**), 1958855 (**8**), 1958861 (**9**), and 1958859 (**10**) contain supplementary crystallographic data for this paper. This information can be obtained free of charge via www.ccdc.cam.ac.uk/data_request/cif or by e-mailing data_request@ccdc.cam.ac.uk or by contacting The Cambridge Crystallographic Data Centre, 12 Union Road, Cambridge CB2 1EZ, U.K.; fax: + 44 1223 336033.

Note

The authors declare no competing financial interest.

References

(1) H. Yersin (Ed.). *Highly Efficient OLEDs: Materials Based on Thermally Activated Delayed Fluorescence*; WILEY- VCH, Weinheim, Germany, 2019.

(2) W. Brütting, C. Adachi (Ed.). *Physics of Organic Semiconductors,* WILEY- VCH, Weinheim, Germany, 2012.

(3) E. Zysman-Colman (Ed.). *Iridium(III) in Optoelectronic and Photonics Applications*; John Wiley and Sons, Chichester, UK, 2017.

(4) H. Yersin (Ed.). *Highly Efficient OLEDs with Phosphorescent Materials*; WILEY-VCH, Weinheim, 2008.

(5) M. A. Baldo, D. F. O'Brien, Y. You, A. Shoustikov, S. Sibley, M. E. Thompson, S. R. Forrest. Highly Efficient Phosphorescent Emission from Organic Electroluminescent Devices. *Nature* **1998**, *395*, 151–154.

(6) Y. Ma, C.-M. Che, H.-Y. Chao, X. Zhou, W.-H. Chan, J. Shen. High Luminescence Gold(I) and Copper(I) Complexes with a Triplet Excited State for Use in Light-Emitting Diodes. *Adv. Mater.* **1999**, *11*, 852–857.

(7) Y. Ma, H. Zhang, J. Shen, C.-M. Che. Electroluminescence from Triplet Metal–Ligand Charge-Transfer Excited State of Transition Metal Complexes. *Synth. Met*. **1998**, *94*, 245–248.

(8) S. Lamansky, P. Djurovich, D. Murphy, F. Abdel-Razzaq, H.-E. Lee, C. Adachi, P. E. Burrows, S. R. Forrest, M. E. Thompson. Highly Phosphorescent Bis-Cyclometalated Iridium Complexes: Synthesis, Photophysical Characterization, and Use in Organic Light Emitting Diodes. *J. Am. Chem. Soc.* **2001**, *123*, 4304–4312.

(9) C. Adachi, M. A. Baldo, M. E. Thompson, S. R. Forrest. Nearly 100% Internal Phosphorescence Efficiency in an Organic Light-Emitting Device. *J. Appl. Phys.* **2001**, *90*, 5048–5051.

(10) N. Armaroli, H. J. Bolink (Eds.). *Photoluminescent Materials and Electroluminescent Devices*; Topics in Current Chemistry Collections, Springer, Cham, Switzerland, 2016.

(11) H. Yersin, A. F. Rausch, R. Czerwieniec, T. Hofbeck, T. Fischer. The Triplet State of Organo-Transition Metal Compounds. Triplet Harvesting and Singlet Harvesting for Efficient OLEDs. *Coord. Chem. Rev.* **2011**, *255*, 2622–2652.

(12) J. C. Deaton, F. N. Castellano. Archetypal Iridium(III) Compounds for Optoelectronic and Photonic Applications: Photophysical Properties and Synthetic Methods. in: E. Zysman-Colman (Ed.), *Iridium(III) in Optoelectronic and Photonics Applications*; Wiley Online Books; John Wiley and Sons, Chichester, UK, 2017; 1–69.

(13) M.-C. Tang, A. K.-W. Chan, M.-Y. Chan, V. W.-W. Yam. Platinum and Gold Complexes for OLEDs. *Top. Curr. Chem.* **2016**, *374*, 1–43.

(14) K. Li, G. S. M. Tong, Q. Wan, G. Cheng, W.-Y. Tong, W.-H. Ang, W.-L. Kwong, C.-M. Che. Highly Phosphorescent Platinum (II) Emitters: Photophysics, Materials and Biological Applications. *Chem. Sci.* **2016**, *7*, 1653-1673.

(15) P.-K. Chow, G. Cheng, G. S. M. Tong, C. Ma, W.-M. Kwok, W.-H. Ang, C. Y.-S. Chung, C. Yang, F. Wang, C.-M. Che. Highly Luminescent Palladium(II) Complexes with Sub-Millisecond Blue to Green Phosphorescent Excited States. Photocatalysis and Highly Efficient PSF-OLEDs. *Chem. Sci.* **2016**, *7*, 6083–6098.

(16) R. Hamze, J. L. Peltier, D. Sylvinson, M. Jung, J. Cardenas, R. Haiges, M. Soleilhavoup, R. Jazzar, P. I. Djurovich, G. Bertrand, M. E. Thompson. Eliminating Nonradiative Decay in Cu(I) Emitters: >99% Quantum Efficiency and Microsecond

Lifetime. *Science* **2019**, *363*, 601–606.

(17) W. Helfrich, W. G. Schneider. Transients of Volume-Controlled Current and of Recombination Radiation in Anthracene. *J. Chem. Phys.* **1966**, *44*, 2902–2909.

(18) H. Yersin. Triplet Emitters for OLED Applications. Mechanisms of Exciton Trapping and Control of Emission Properties. *Top. Curr. Chem.* **2004**, *241*, 1–26.

(19) C. W. Tang, S. A. VanSlyke. Organic Electroluminescent Diodes. *Appl. Phys. Lett.* **1987**, *51*, 913–915.

(20) C.-M. Che, C.-C. Kwok, S.-W. Lai, A. F. Rausch, W. J. Finkenzeller, N. Zhu, H. Yersin. Photophysical Properties and OLED Applications of Phosphorescent Platinum(II) Schiff Base Complexes. *Chem. – A Eur. J.* **2010**, *16*, 233–247.

(21) Y.-Y. Lin, S.-C. Chan, M. C. W. Chan, Y.-J. Hou, N. Zhu, C.-M. Che, Y. Liu, Y. Wang. Structural, Photophysical, and Electrophosphorescent Properties of Platinum(II) Complexes Supported by Tetradentate N_2O_2 Chelates. *Chem. – A Eur. J.* **2003**, *9*, 1263–1272.

(22) G. Cheng, S. C. F. Kui, W.-H. Ang, M.-Y. Ko, P.-K. Chow, C.-L. Kwong, C.-C. Kwok, C. Ma, X. Guan, K.-H. Low, S.-J. Su, C.-M. Che. Structurally Robust Phosphorescent [Pt(O^N^C^N)] Emitters for High Performance Organic Light-Emitting Devices with Power Efficiency up to 126 lm W^{-1} and External Quantum Efficiency over 20%. *Chem. Sci.* **2014**, *5*, 4819–4830.

(23) M. Mao, J. Peng, T.-L. Lam, W.-H. Ang, H. Li, G. Cheng, C.-M. Che. High-Performance Organic Light-Emitting Diodes with Low-Efficiency Roll-off Using Bulky Tetradentate [Pt (O^ N^ C^ N)] Emitters. *J. Mater. Chem. C* **2019**, *7*, 7230–7236.

(24) G. Cheng, Y. Kwak, W.-P. To, T.-L. Lam, G. S. M. Tong, M.-K. Sit, S. Gong, B. Choi, W. i. Choi, C. Yang, C.-M. Che. High-Efficiency Solution-Processed Organic Light-Emitting Diodes with Tetradentate Platinum(II) Emitters. *ACS Appl. Mater. Interfaces* **2019**, *11*, 45161−45170.

(25) D. A. K. Vezzu, J. C. Deaton, J. S. Jones, L. Bartolotti, C. F. Harris, A. P. Marchetti, M. Kondakova, R. D. Pike, S. Huo. Highly Luminescent Tetradentate Bis-Cyclometalated Platinum Complexes: Design, Synthesis, Structure, Photophysics, and Electroluminescence Application. *Inorg. Chem.* **2010**, *49*, 5107–5119.

(26) T. Fleetham, G. Li, L. Wen, J. Li. Efficient "Pure" Blue OLEDs Employing Tetradentate Pt Complexes with a Narrow Spectral Bandwidth. *Adv. Mater.* **2014**, *26*, 7116–7121.

(27) H. Yersin, A. F. Rausch, R. Czerwieniec. Organometallic Emitters for OLEDs: Triplet Harvesting, Singlet Harvesting, Case Structures, and Trends. in: W. Brütting, C. Adachi (Eds.), *Physics of Organic Semiconductors*; Wiley-VCH, Weinheim, Germany, 2012; 371–424.

(28) H. Yersin, W. J. Finkenzeller. Triplet Emitters for Organic Light-Emitting Diodes : Basic Properties. In: *Highly Efficient OLEDs with Phosphorescent Materials*; Yersin (Ed.), Wiley-VCH, Weinheim, Germany, 2008; 1–97.

(29) H. Yersin, U. Monkowius. Komplexe Mit kleinen Singulett-Triplett-Energie-Abständen Zur Verwendung in Opto-Elektronischen Bauteilen (Singulett-Harvesting-Effekt). DE102008033563 (2008), Internal Invention Disclosure, University of Regensburg, Germany, 2006.

(30) R. Czerwieniec, J. Yu, H. Yersin. Blue-Light Emission of Cu(I) Complexes and Singlet Harvesting. *Inorg. Chem.* **2011**, *50*, 8293–8301.

(31) J. C. Deaton, S. C. Switalski, D. Y. Kondakov, R. H. Young, T. D. Pawlik, D. J. Giesen, S. B. Harkins, A. J. M. Miller, S. F. Mickenberg, J. C. Peters. E-Type Delayed Fluorescence of a Phosphine-Supported $Cu_2(\mu\text{-}NAr_2)_2$ Diamond Core: Harvesting Singlet and Triplet Excitons in OLEDs. *J. Am. Chem. Soc.* **2010**, *132*, 9499–9508.

(32) R. Czerwieniec, H. Yersin. Diversity of Copper(I) Complexes Showing Thermally Activated Delayed Fluorescence: Basic Photophysical Analysis. *Inorg. Chem.* **2015**, *54*, 4322–4327.

(33) D. M. Zink, D. Volz, T. Baumann, M. Mydlak, H. Flügge, J. Friedrichs, M. Nieger, S. Bräse. Heteroleptic, Dinuclear Copper(I) Complexes for Application in Organic Light-Emitting Diodes. *Chem. Mater.* **2013**, *25*, 4471–4486.

(34) F. Dumur. Recent Advances in Organic Light-Emitting Devices Comprising Copper Complexes: A Realistic Approach for Low-Cost and Highly Emissive Devices? *Org. Electron.* **2015**, *21*, 27–39.

(35) M. Osawa, M. Hoshino, M. Hashimoto, I. Kawata, S. Igawa, M. Yashima. Application of Three-Coordinate Copper(I) Complexes with Halide Ligands in Organic Light-Emitting Diodes that Exhibit Delayed Fluorescence. *Dalt. Trans.* **2015**, *44*, 8369–8378.

(36) R. Yu, C.-Z. Lu. Ionic $[Cu(NN)(PP)]^+$ TADF Complexes with Pyridine-Based Diimine Chelating Ligands and their Use in OLEDs. In: *Highly Efficient OLEDs - Materials Based on Thermally Activated Delayed Fluorescence*. H. Yersin. (Ed.), WILEY- VCH, Weinheim, Germany 2019, pp 177–198.

(37) M. J. Leitl, D. M. Zink, A. Schinabeck, T. Baumann, D. Volz, H. Yersin. Copper(I) Complexes for Thermally Activated Delayed Fluorescence: From Photophysical to Device Properties. *Top. Curr. Chem.* **2016**, *374*, 25.

(38) R. Czerwieniec, M. J. Leitl, H. H. H. Homeier, H. Yersin. Cu(I) Complexes – Thermally Activated Delayed Fluorescence. Photophysical Approach and Material Design. *Coord. Chem. Rev.* **2016**, *325*, 2–28.

(39) G. K.-M. So, G. Cheng, J. Wang, X. Chang, C.-C. Kwok, H. Zhang, C.-M. Che. Efficient Color-Tunable Copper(I) Complexes and Their Applications in Solution-Processed Organic Light-Emitting Diodes. *Chem. – An Asian J.* **2017**, *12*, 1490–1498.

(40) D. M. Zink, M. Bächle, T. Baumann, M. Nieger, M. Kühn, C. Wang, W. Klopper, U. Monkowius, T. Hofbeck, H. Yersin, S. Bräse. Synthesis, Structure, and Characterization of Dinuclear Copper(I) Halide Complexes with P^N Ligands Featuring Exciting Photoluminescence Properties. *Inorg. Chem.* **2013**, *52*, 2292–2305.

(41) M. Wallesch, D. Volz, D. M. Zink, U. Schepers, M. Nieger, T. Baumann, S. Bräse. Bright Coppertunities: Multinuclear CuI Complexes with N-P Ligands and Their Applications. *Chem. -- A Eur. J.* **2014**, *20*, 6578–6590.

(42) C. Bizzarri, F. Hundemer, J. Busch, S. Bräse. Triplet Emitters versus TADF Emitters in OLEDs: A Comparative Study. *Polyhedron* **2018**, *140*, 51–66.

(43) A. V Artem'ev, M. R. Ryzhikov, I. V Taidakov, M. I. Rakhmanova, E. A. Varaksina, I. Y. Bagryanskaya, S. F. Malysheva, N. A. Belogorlova. Bright Green-to-Yellow Emitting Cu(I) Complexes Based on Bis(2-Pyridyl)Phosphine Oxides: Synthesis, Structure and Effective Thermally Activated-Delayed Fluorescence. *Dalt. Trans.* **2018**, *47*, 2701–2710.

(44) H. Ohara, A. Kobayashi, M. Kato. Effects of N-Heteroaromatic Ligands on Highly Luminescent Mononuclear Copper(I)–Halide Complexes. *Comptes Rendus Chim.* **2015**, *18*, 766–775.

(45) H. Ohara, A. Kobayashi, M. Kato. Simple and Extremely Efficient Blue Emitters Based on Mononuclear Cu(I)-Halide Complexes with Delayed Fluorescence. *Dalt. Trans.* **2014**, *43*, 17317–17323.

(46) K. Nozaki, M. Iwamura. Highly Emissive d^{10} Metal Complexes as TADF Emitters with Versatile Structures and Photophysical Properties. in: H. Yersin (Ed.), *Highly Efficient OLEDs - Materials Based on Thermally Activated Delayed Fluorescence*; WILEY-VCH, Weinheim, Germany, 2019; 61–91.

(47) A. Tsuboyama. Luminescent Dinuclear Copper(I) Complexes with Short Intramolecular Cu–Cu Distances. in: H. Yersin (Ed.), *Highly Efficient OLEDs - Materials Based on Thermally Activated Delayed Fluorescence*; WILEY- VCH, Weinheim, Germany, 2019; 93–118.

(48) M. Osawa, M. Hoshino. Molecular Design and Synthesis of Metal Complexes as Emitters for TADF-Type OLEDs. in: H. Yersin (Ed.), *Highly Efficient OLEDs - Materials Based on Thermally Activated Delayed Fluorescence*; WILEY- VCH, Weinheim, Germany, 2019; 119–176.

(49) H. Yersin, R. Czerwieniec, M. Z. Shafikov, A. F. Suleymanova. TADF Material Design: Photophysical Background and Case Studies Focusing on Cu(I) and Ag(I) Complexes. *ChemPhysChem* **2017**, *18*, 3508–3535.

(50) L. Bergmann, D. M. Zink, S. Bräse, T. Baumann, D. Volz. Metal–Organic and Organic TADF-Materials: Status, Challenges and Characterization.Top. Curr. Chem. **2016**, *374,* 22.

(51) N. Armaroli, G. Accorsi, F. Cardinali, A. Listorti. Photochemistry and Photophysics of Coordination Compounds: Copper - Photochemistry. *Top. Curr. Chem.* **2007**, *280*, 69–115.

(52) M. J. Leitl, F.-R. Küchle, H. A. Mayer, L. Wesemann, H. Yersin. Brightly Blue and Green Emitting Cu(I) Dimers for Singlet Harvesting in OLEDs. *J. Phys. Chem. A* **2013**, *117*, 11823–11836.

(53) X.-L. Chen, R. Yu, X.-Y. Wu, D. Liang, J.-H. Jia, C.-Z. Lu. A Strongly Greenish-Blue-Emitting Cu_4Cl_4 Cluster with an Efficient Spin–Orbit Coupling (SOC): Fast Phosphorescence versus Thermally Activated Delayed Fluorescence. *Chem. Commun.* **2016**, *52*, 6288–6291.

(54) C. L. Linfoot, M. J. Leitl, P. Richardson, A. F. Rausch, O. Chepelin, F. J. White, H.

Yersin, N. Robertson. Thermally Activated Delayed Fluorescence (TADF) and Enhancing Photoluminescence Quantum Yields of [Cu(I)(Diimine)(Diphosphine)]$^+$ Complexes—Photophysical, Structural, and Computational Studies. *Inorg. Chem.* **2014**, *53*, 10854–10861.

(55) A. Schinabeck, M. J. Leitl, H. Yersin. Dinuclear Cu(I) Complex with Combined Bright TADF and Phosphorescence. Zero-Field Splitting and Spin–Lattice Relaxation Effects of the Triplet State. *J. Phys. Chem. Lett.* **2018**, *9*, 2848–2856.

(56) S. Igawa, M. Hashimoto, I. Kawata, M. Yashima, M. Hoshino, M. Osawa. Highly Efficient Green Organic Light-Emitting Diodes Containing Luminescent Tetrahedral Copper(I) Complexes. *J. Mater. Chem. C* **2013**, *1*, 542–551.

(57) T. Gneuß, M. J. Leitl, L. H. Finger, N. Rau, H. Yersin, J. Sundermeyer. A New Class of Luminescent Cu(I) Complexes with Tripodal Ligands – TADF Emitters for the Yellow to Red Color Range. *Dalt. Trans.* **2015**, *44*, 8506–8520.

(58) A. Schinabeck, N. Rau, M. Klein, J. Sundermeyer, H. Yersin. Deep Blue Emitting Cu(I) Tripod Complexes. Design of High Quantum Yield Materials Showing TADF-Assisted Phosphorescence. *Dalt. Trans.* **2018**, *47*, 17067–17076.

(59) A. Schinabeck, J. Chen, L. Kang, T. Teng, H. H. H. Homeier, A. F. Suleymanova, M. Z. Shafikov, R. Yu, C.-Z. Lu, H. Yersin. Symmetry-Based Design Strategy for Unprecedentedly Fast Decaying Thermally Activated Delayed Fluorescence (TADF). Application to Dinuclear Cu(I) Compounds. *Chem. Mater.* **2019**, *31*, 4392–4404.

(60) S. Shi, M. C. Jung, C. Coburn, A. Tadle, D. Sylvinson M. R., P. I. Djurovich, S. R. Forrest, M. E. Thompson. Highly Efficient Photo- and Electroluminescence from Two-Coordinate Cu(I) Complexes Featuring Nonconventional N-Heterocyclic Carbenes. *J. Am. Chem. Soc.* **2019**, *141*, 3576–3588.

(61) R. Hamze, S. Shi, S. C. Kapper, D. S. Muthiah Ravinson, L. Estergreen, M.-C. Jung, A. C. Tadle, R. Haiges, P. I. Djurovich, J. L. Peltier, R. Jazzar, G. Bertrand, S. E. Bradforth, M. E. Thompson. "Quick-Silver" from a Systematic Study of Highly Luminescent, Two-Coordinate, d^{10} Coinage Metal Complexes. *J. Am. Chem. Soc.* **2019**, *141*, 8616–8626.

(62) M. Z. Shafikov, A. F. Suleymanova, R. Czerwieniec, H. Yersin. Design Strategy for Ag(I)-Based Thermally Activated Delayed Fluorescence Reaching an Efficiency Breakthrough. *Chem. Mater.* **2017**, *29*, 1708–1715.

(63) M. Z. Shafikov, A. F. Suleymanova, A. Schinabeck, H. Yersin. Dinuclear Ag(I) Complex Designed for Highly Efficient Thermally Activated Delayed Fluorescence. *J. Phys. Chem. Lett.* **2018**, *9*, 702–709.

(64) M. Osawa, I. Kawata, R. Ishii, S. Igawa, M. Hashimoto, M. Hoshino. Application of Neutral d^{10} Coinage Metal Complexes with an Anionic Bidentate Ligand in Delayed Fluorescence-Type Organic Light-Emitting Diodes. *J. Mater. Chem. C* **2013**, *1*, 4375–4383.

(65) J. Chen, T. Teng, L. Kang, X.-L. Chen, X.-Y. Wu, R. Yu, C.-Z. Lu. Highly Efficient Thermally Activated Delayed Fluorescence in Dinuclear Ag(I) Complexes with a Bis-Bidentate Tetraphosphane Bridging Ligand. *Inorg. Chem.* **2016**, *55*, 9528–9536.

(66) X.-M. Gan, R. Yu, X.-L. Chen, M. Yang, L. Lin, X.-Y. Wu, C.-Z. Lu. A Unique Tetranuclear Ag(I) Complex Emitting Efficient Thermally Activated Delayed Fluorescence with a Remarkably Short Decay Time. *Dalt. Trans.* **2018**, *47*, 5956–5960.

(67) G. K.-M. So, G. Cheng, J. Wang, X. Chang, C.-C. Kwok, H. Zhang, C.-M. Che. Efficient Color-Tunable Copper(I) Complexes and Their Applications in Solution-Processed Organic Light-Emitting Diodes. *Chem. – An Asian J.* **2017**, *12*, 1490–1498.

(68) T. Gneuß, M. J. Leitl, L. H. Finger, H. Yersin, J. Sundermeyer A new class of deep-blue emitting Cu(I) compounds – effects of counter ions on the emission behavior. *Dalton Trans.,* **2015***, 44,* 20045–20055.

(69) A. Y. Baranov, A. S. Berezin, D. G. Samsonenko, A. S. Mazur, P. M. Tolstoy, V. F. Plyusnin, I. E. Kolesnikov, A. V. Artem'ev, New Cu(I) halide complexes showing TADF combined with room temperature phosphorescence: the balance tuned by halogens. *Dalton Trans.,* **2020***, 49,* 3155–3163.

(70) K.-T. Chan, T.-L. Lam, D. Yu, L. Du, D. L. Phillips, C.-L. Kwong, G. S. M. Tong, G. Cheng, C.-M. Che. Strongly Luminescent Tungsten Emitters with Emission Quantum Yields of up to 84%: TADF and High-Efficiency Molecular Tungsten OLEDs. *Angew. Chem. Int. Ed.* **2019**, *58*, 14896 –14900.

(71) J. Fernandez-Cestau, B. Bertrand, M. Blaya, G. A. Jones, T. J. Penfold, M. Bochmann. Synthesis and Luminescence Modulation of Pyrazine-Based Gold(III) Pincer Complexes. *Chem. Commun.*, **2015**, *51*, 16629–16632.

(72) W.-P. To, D. Zhou, G. S. M. Tong, G. Cheng, C. Yang, C.-M. Che. Highly Luminescent Pincer Gold(III) Aryl Emitters: Thermally Activated Delayed Fluorescence and Solution-Processed OLEDs. *Angew. Chem. Int. Ed.* **2017**, *56*, 14036 –14041.

(73) D. Zhou, W.-P. To, Y. Kwak, Y. Cho, G. Cheng, G. S. M. Tong, C.-M. Che. Thermally Stable Donor–Acceptor Type (Alkynyl)Gold(III) TADF Emitters Achieved EQEs and Luminance of up to 23.4% and 70 300 cd m^{-2} in Vacuum-Deposited OLEDs. *Adv. Sci.* **2019**, *6*, 1802297.

(74) D. Zhou,W.-P. To, G. S. M. Tong, G. Cheng, L. Du, D. L. Phillips, C.-M. Che. Tetradentate Gold(III) Complexes as Thermally Activated Delayed Fluorescence (TADF) Emitters: Microwave-Assisted Synthesis and High-Performance OLEDs with Long Operational Lifetime. *Angew. Chem. Int. Ed.* **2020**, *59*, 6375–6382.

(75) L.-K. Li, M.-C. Tang, S.-L. Lai, M. Ng, W.-K. Kwok, M.-Y. Chan, V. W.-W. Yam. Strategies Towards Rational Design of Gold(III) Complexes for High-Performance Organic Light-Emitting Devices. *Nat. Photonics* **2019**, *13*, 185–191.

(76) C.-H. Lee, M.-C. Tang, F. K.-W. Kong, W.-L. Cheung, M. Ng, M.-Y. Chan, V. W.-W. Yam. Isomeric Tetradentate Ligand-Containing Cyclometalated Gold(III) Complexes. *J. Am. Chem. Soc.* **2020**, *142*, 520−529.

(77) D. Di, A. S. Romanov, L. Yang, J. M. Richter, J. P. H. Rivett, S. Jones, T. H. Thomas,M. A. Jalebi, R. H. Friend, M. Linnolahti, M. Bochmann, D. Credgington. High-Performance Light-Emitting Diodes Based on Carbene-Metal-Amides. *Science* **2017**, *356*, 159–163.

(78) P. J. Conaghan, S. M. Menke, A. S. Romanov, S. T. E. Jones, A. J. Pearson, E. W. Evans, M. Bochmann, N. C. Greenham, D. Credgington. Efficient Vacuum-Processed Light-Emitting Diodes Based on Carbene–Metal–Amides. *Adv. Mater.* **2018**, *30*, 1802285.

(79) H. Uoyama, K. Goushi, K. Shizu, H. Nomura, C. Adachi. Highly Efficient Organic Light-Emitting Diodes from Delayed Fluorescence. *Nature* **2012**, *492*, 234–238.

(80) T. Hosokai, H. Matsuzaki, H. Nakanotani, K. Tokumaru, T. Tsutsui, A. Furube, K. Nasu, H. Nomura, M. Yahiro, C. Adachi. Evidence and Mechanism of Efficient Thermally Activated Delayed Fluorescence Promoted by Delocalized Excited States. *Sci. Adv.* **2017**, *3*.

(81) Y. Liu, C. Li, Z. Ren, S. Yan, M. R. Bryce. All-Organic Thermally Activated Delayed Fluorescence Materials for Organic Light-Emitting Diodes. *Nat. Rev. Mater.* **2018**, *3*, 18020.

(82) R. Komatsu, T. Ohsawa, H. Sasabe, K. Nakao, Y. Hayasaka, J. Kido. Manipulating the Electronic Excited State Energies of Pyrimidine-Based Thermally Activated Delayed Fluorescence Emitters to Realize Efficient Deep-Blue Emission. *ACS Appl. Mater. Interfaces* **2017**, *9*, 4742–4749.

(83) M. Li, Y. Liu, R. Duan, X. Wei, Y. Yi, Y. Wang, C.-F. Chen. Aromatic-Imide-Based Thermally Activated Delayed Fluorescence Materials for Highly Efficient Organic Light-Emitting Diodes. *Angew. Chemie Int. Ed.* **2017**, *56*, 8818–8822.

(84) N. Sharma, M. Y. Wong, I. D. W. Samuel, E. Zysman-Colman. Solution-Processed TADF Materials and Devices Based on Organic Emitters. in: H. Yersin (Ed.), *Highly Efficient OLEDs - Materials Based on Thermally Activated Delayed Fluorescence*; WILEY- VCH, Weinheim, Germany, 2019; 501–541.

(85) M. Y. Wong, E. Zysman-Colman. Purely Organic Thermally Activated Delayed Fluorescence Materials for Organic Light-Emitting Diodes. *Adv. Mater.* **2017**, *29*, 1605444.

(86) G. A. Sommer, L. N. Mataranga-Popa, R. Czerwieniec, T. Hofbeck, H. H. H. Homeier, T. J. J. Müller, H. Yersin. Design of Conformationally Distorted Donor–Acceptor Dyads Showing Efficient Thermally Activated Delayed Fluorescence. *J. Phys. Chem. Lett.* **2018**, *9*, 3692–3697.

(87) T. D. Schmidt, W. Brütting. Efficiency Enhancement of Organic Light-Emitting Diodes Exhibiting Delayed Fluorescence and Nonisotropic Emitter Orientation. in: H. Yersin (Ed.), *Highly Efficient OLEDs - Materials Based on Thermally Activated Delayed Fluorescence*; WILEY- VCH, Weinheim, Germany, 2019; 199–228.

(88) A. Arjona-Esteban, D. Volz. Status and Next Steps of TADF Technology: An Industrial Perspective. In: *Highly Efficient OLEDs - Materials Based on Thermally Activated Delayed Fluorescence*; H. Yersin (Ed.), WILEY- VCH, Weinheim, Germany, 2019; pp 543–572.

(89) X.-K. Chen, D. Kim, J.-L. Brédas. Thermally Activated Delayed Fluorescence (TADF) Path toward Efficient Electroluminescence in Purely Organic Materials: Molecular Level Insight. *Acc. Chem. Res.* **2018**, *51*, 2215–2224.

(90) C. A. Parker, C. G. Hatchard. Triplet-Singlet Emission in Fluid Solutions. Phosphorescence of Eosin. *Trans. Faraday Soc.* **1961**, *57*, 1894–1904.

(91) H. Yersin, L. Mataranga-Popa, R. Czerwieniec, Y. Dovbii. Design of a New Mechanism beyond Thermally Activated Delayed Fluorescence toward Fourth Generation Organic Light Emitting Diodes. *Chem. Mater.* **2019**, *31*, 6110–6116.

(92) H. Yersin, L. Mataranga-Popa, S.-W. Li, R. Czerwieniec. Design Strategies for Materials Showing Thermally Activated Delayed Fluorescence and beyond: Towards the Fourth-Generation OLED Mechanism. *J. Soc. Inf. Disp.* **2018**, *26*, 194–199.

(93) H. Yersin; L. Mataranga-Popa; R. Czerwieniec. European Patent EP 3 401 381 A1, 2017; German Patent DE 10 2017 101 432 A1, 2017; US patent: US 2019/0245151A1.

(94) H. Yersin; German Patent DE 10 2020 103 268.4, **2020**.

(95) H. Noda, H. Nakanotani, C. Adachi. Excited State Engineering for Efficient Reverse Intersystem Crossing. *Sci. Adv.* **2018**, *4*, eaao6910.

(96) L. X. Chen, G. B. Shaw, I. Novozhilova, T. Liu, G. Jennings, K. Attenkofer, G. J. Meyer, P. Coppens. MLCT State Structure and Dynamics of a Copper(I) Diimine Complex Characterized by Pump−Probe X-Ray and Laser Spectroscopies and DFT Calculations. *J. Am. Chem. Soc.* **2003**, *125*, 7022–7034.

(97) Z. A. Siddique, Y. Yamamoto, T. Ohno, K. Nozaki. Structure-Dependent Photophysical Properties of Singlet and Triplet Metal-to-Ligand Charge Transfer States in Copper(I) Bis(Diimine) Compounds. *Inorg. Chem.* **2003**, *42*, 6366–6378.

(98) M. Iwamura, S. Takeuchi, T. Tahara. Real-Time Observation of the Photoinduced Structural Change of Bis(2,9-Dimethyl-1,10-Phenanthroline)Copper(I) by Femtosecond Fluorescence Spectroscopy: A Realistic Potential Curve of the Jahn−Teller Distortion. *J. Am. Chem. Soc.* **2007**, *129*, 5248–5256.

(99) N. J. Turro. *Modern Molecular Photochemistry of Organic Molecules.* Benjamin/Cummings, Melon Park, California, 1978.

(100) S. Igawa, M. Hashimoto, I. Kawata, M. Hoshino, M. Osawa. Photoluminescence Properties, Molecular Structures, and Theoretical Study of Heteroleptic Silver(I) Complexes Containing Diphosphine Ligands. *Inorg. Chem.* **2012**, *51*, 5805–5813.

(101) C. M. Reisinger, R. J. Nowack, D. Volkmer, B. Rieger. Novel Palladium Complexes Employing Mixed Phosphine Phosphonates and Phosphine Phosphinates as Anionic Chelating [P,O] Ligands. *Dalt. Trans.* **2007**, No. 2, 272–278.

(102) T. A. Van Der Knaap, T. C. Klebach, F. Visser, R. Lourens, F. Bickelhaupt. [4+2]Cycloaddition Reactions of Triarylphosphaalkene. *Tetrahedron* **1984**, *40*, 991–997.

(103) R. D. Shannon. Revised Effective Ionic Radii and Systematic Studies of Interatomic Distances in Halides and Chalcogenides. *Acta Crystallogr. Sect. A* **1976**, *32*, 751–767.

(104) R. G. Pearson. Hard and Soft Acids and Bases. *J. Am. Chem. Soc.* **1963**, *85*, 3533–3539.

(105) P. Strauch, W. Dietzsch, L. Golič. Photolysereaktionen an Thiooxalat-

Zweikernkomplexen – Kristall- und Molekülstruktur von Hydrogensulfidopyridinbis(Triphenylphosphan)Kupfer(I). *Zeitschrift für Anorg. und Allg. Chemie* **1997**, *623*, 129–134.

(106) L. M. Engelhardt, P. C. Healy, J. D. Kildea, A. H. White. Lewis-Base Adducts of Group 11 Metal(I) Compounds. LI. Synthesis and Structural Characterization of Mononuclear Chloro-, Bromo- and Iodo Pyridinebis(Triphenylphosphine)Copper(I) Complexes. *Aust. J. Chem.* **1989**, *42*, 895–905.

(107) M. Camalli, F. Caruso. Correlation between ^{31}P NMR Data and Structural Parameters on $Ag(PPh_3)_3X$ Series. Crystal and Molecular Structure of Tris(Triphenylphosphine)Silver(I)Tetrafluoroborate and Tris(Triphenylphosphine)Silver(I)Iodide. *Inorganica Chim. Acta* **1987**, *127*, 209–213.

(108) J. Chen, T. Teng, L. Kang, X.-L. Chen, X.-Y. Wu, R. Yu, C.-Z. Lu. Highly Efficient Thermally Activated Delayed Fluorescence in Dinuclear Ag(I) Complexes with a Bis-Bidentate Tetraphosphane Bridging Ligand. *Inorg. Chem.* **2016**, *55*, 9528–9536.

(109) H. Yersin, M. J. Leitl, R. Czerwieniec. TADF for Singlet Harvesting: Next Generation OLED Materials Based on Brightly Green and Blue Emitting Cu(I) and Ag(I) Compounds. in *Proc.SPIE-The International Society for Optical Engineering*, SPIE, Bellingham, WA, 2014; Vol. 9183.

(110) A. Kaeser, O. Moudam, G. Accorsi, I. Séguy, J. Navarro, A. Belbakra, C. Duhayon, N. Armaroli, B. Delavaux-Nicot, J.-F. Nierengarten. Homoleptic Copper(I), Silver(I), and Gold(I) Bisphosphine Complexes. *Eur. J. Inorg. Chem.* **2014**, *2014*, 1345–1355.

(111) C.-W. Hsu, C.-C. Lin, M.-W. Chung, Y. Chi, G.-H. Lee, P.-T. Chou, C.-H. Chang, P.-Y. Chen. Systematic Investigation of the Metal-Structure–Photophysics Relationship of Emissive d^{10}-Complexes of Group 11 Elements: The Prospect of Application in Organic Light Emitting Devices. *J. Am. Chem. Soc.* **2011**, *133*, 12085–12099.

(112) C.-C. Hsu, C.-C. Lin, P.-T. Chou, C.-H. Lai, C.-W. Hsu, C.-H. Lin, Y. Chi. Harvesting Highly Electronically Excited Energy to Triplet Manifolds: State-Dependent Intersystem Crossing Rate in Os(II) and Ag(I) Complexes. *J. Am. Chem. Soc.* **2012**, *134*, 7715–7724.

(113) H. Kunkely, A. Vogler. Optical Properties of Ag(Tripod)X with Tripod=1,1,1-Tris(Diphenyl-Phosphinomethyl)Ethane and X^-=Cl^- and I^-: Intraligand and Ligand-to-Ligand Charge Transfer. *Inorg. Chim. Acta* **2006**, *359*, 388–390.

(114) M. Z. Shafikov, R. Czerwieniec, H. Yersin. Ag(I) Complex Design Affording Intense Phosphorescence with a Landmark Lifetime of over 100 Milliseconds. *Dalt. Trans.* **2019**, *48*, 2802–2806.

(115) H. L. Schläfer, G. Gliemann, *Einführung in die Ligandenfeldtheorie*. Akademische Verlagsgesellschaft, Frankfurt am Main,1967.

(116) U. Rössler, H. Yersin. Destabilization of a Self-Trapped Exciton in a Quasi-One-

Dimensional Semiconductor: $Mg[Pt(CN)_4]\cdot 7H_2O$ with Hydrostatic Pressure. *Phys. Rev. B* **1982**, *26*, 3187–3191.

(117) G. Gliemann, H. Yersin. Spectroscopic Properties of the Quasi One-Dimensional Tetracyanoplatinate(II) Compounds. *Struct. Bond.* **1985**, *62*, 87–153.

(118) A. F. Rausch, M. E. Thompson, H. Yersin. Matrix Effects on the Triplet State of the OLED Emitter $Ir(4,6\text{-}dFppy)_2(pic)$ (FIrpic): Investigations by High-Resolution Optical Spectroscopy. *Inorg. Chem.* **2009**, *48*, 1928–1937.

(119) D. R. Striplin, G. A. Crosby. Nature of the Emitting ^{3}MLCT Manifold of $Rhenium(I)(diimine)(CO)_3Cl$ Complexes. *Chem. Phys. Lett.* **1994**, *221*, 426–430.

(120) L. Bergmann, G. J. Hedley, T. Baumann, S. Bräse, I. D. W. Samuel. Direct Observation of Intersystem Crossing in a Thermally Activated Delayed Fluorescence Copper Complex in the Solid State. *Sci. Adv.* **2016**, *2*, e1500889.

(121) H. Yersin, J. Strasser. Triplets in Metal–Organic Compounds. Chemical Tunability of Relaxation Dynamics. *Coord. Chem. Rev.* **2000**, *208*, 331–364.

(122) H. Yersin, D. Donges. Low-Lying Electronic States and Photophysical Properties of Organometallic Pd(II) and Pt(II) Compounds. Modern Research Trends Presented in Detailed Case Studies. *Top. Curr. Chem.* **2001**, *214*, 81–186.

(123) D. S. Tinti, M. A. El-Sayed. New Techniques in Triplet State Phosphorescence Spectroscopy: Application to the Emission of 2,3-Dichloroquinoxaline. *J. Chem. Phys.* **1971**, *54*, 2529–2549.

(124) J. Schmidt, H. Wiedenhofer, A. von Zelewsky, H. Yersin. Time-Resolved Vibrational Structures of the Triplet Sublevel Emission of $Pd(2\text{-}thpy)_2$. *J. Phys. Chem.* **1995**, *99*, 226–229.

(125) H. Yersin, D. Donges, J. K. Nagle, R. Sitters, M. Glasbeek. Intraligand Charge Transfer in the Pd(II) Oxinate Complex $Pd(qol)_2$. Site-Selective Emission, Excitation, and Optically Detected Magnetic Resonance. *Inorg. Chem.* **2000**, *39*, 770–777.

(126) M. A. El-Sayed. Spin-Orbit Coupling and the Radiationless Processes in Nitrogen Heterocyclics. *J. Chem. Phys.* **1963**, *38*, 2834–2838.

(127) A. F. Rausch, H. H. H. Homeier, H. Yersin. Organometallic Pt(II) and Ir(III) Triplet Emitters for OLED Applications and the Role of Spin–Orbit Coupling: A Study Based on High-Resolution Optical Spectroscopy. *Top. Organomet. Chem*. **2010**, *29*,193–235.

(128) S. P. McGlynn, M. Kinoshita, T. Azumi. *Molecular Spectroscopy of the Triplet State*, Englewood Cliffs, N.J., Prentice-Hall, 1969.

(129) H. Wiedenhofer, S. Schuetzenmeier, A. von Zelewsky, H. Yersin. Characterization of Triplet Sublevels by Highly Resolved Vibrational Satellite Structures. Application to $Pt(2\text{-}thpy)_2$. *J. Phys. Chem.* **1995**, *99*, 13385–13391.

(130) T. Hofbeck, Y. C. Lam, M. Kalbáč, S. Záliš, A. Vlček, H. Yersin. Thermally Tunable Dual Emission of the d^8–d^8 Dimer $[Pt_2(\mu\text{-}P_2O_5(BF_2)_2)_4]^{4-}$. *Inorg. Chem.* **2016**, *55*, 2441–2449.

(131) T. J. Penfold, E. Gindensperger, C. Daniel, C. M. Marian. Spin-Vibronic Mechanism for Intersystem Crossing. *Chem. Rev.* **2018**, *118*, 6975–7025.

(132) R. J. Holmes, B. W. D'Andrade, S. R. Forrest, X. Ren, J. Li, M. E. Thompson. Efficient, Deep-Blue Organic Electrophosphorescence by Guest Charge Trapping. *Appl. Phys. Lett.* **2003**, *83*, 3818–3820.

(133) M. Uchida, C. Adachi, T. Koyama, Y. Taniguchi. Charge Carrier Trapping Effect by Luminescent Dopant Molecules in Single-Layer Organic Light Emitting Diodes. *J. Appl. Phys.* **1999**, 86, 1680–1687.

(134) Y. Liu, S.-C. Yiu, C.-L. Ho, W.-Y. Wong. Recent Advances in Copper Complexes for Electrical/Light Energy Conversion. *Coord. Chem. Rev.* **2018**, *375*, 514–557.

(135) F. Zhang, Y. Guan, X. Chen, S. Wang, D. Liang, Y. Feng, S. Chen, S. Li, Z. Li, F. Zhang, C. Lu, G. Cao, B. Zhai. Syntheses, Photoluminescence, and Electroluminescence of a Series of Sublimable Bipolar Cationic Cuprous Complexes with Thermally Activated Delayed Fluorescence. *Inorg. Chem.* **2017**, *56*, 3742−3753.

(136) J. Zhang, C. Duan, C. Han, H. Yang, Y. Wei, H. Xu. Balanced Dual Emissions from Tridentate Phosphine Coordinate Copper(I) Complexes toward Highly Efficient Yellow OLEDs. *Adv. Mater.* **2016**, *28*, 5975–5979.